2017-08-01

Post-Translational Regulation of Superoxide Dismutase 1 (SOD1): The Effect of K122 Acylation on SOD1's Metabolic Activity

Courtney Jean Banks
Brigham Young University

Post-Translational Regulation of Superoxide Dismutase 1 (SOD1):

The Effect of K122 Acylation on SOD1's Metabolic Activity

Courtney Jean Banks

A dissertation submitted to the faculty of
Brigham Young University
in partial fulfillment of the requirements for the degree of

Doctor of Philosophy

Joshua Andersen, Chair
Benjamin Thomas Bikman
Kenneth A. Christensen
Richard Kent Watt
Barry M. Willardson

Department of Chemistry and Biochemistry

Brigham Young University

ABSTRACT

Post-Translational Regulation of Superoxide Dismutase 1 (SOD1):
The Effect of K122 Acylation on SOD1's Metabolic Activity

Courtney Jean Banks
Department of Chemistry and Biochemistry, BYU
Doctor of Philosophy

Many mutations in superoxide dismutase 1 (SOD1) cause destabilization and misfolding of the protein and are implicated in amyotrophic lateral sclerosis. Likewise, a few post-translational modifications (PTMs) on SOD1 have been shown to cause the same phenotype. However, relatively few PTMs on SOD1 have been studied in depth and, in particular, very few studies have demonstrated how these PTMs affect SOD1's various biological roles. SOD1 is traditionally known for its role in reactive oxygen species (ROS)-scavenging but has also been found to have a few other biological roles, including transcription factor activity to promote genomic stability, preservation of cytoskeletal activity, maintaining zinc and copper homeostasis, and suppressing respiration. We have used the computational analysis tool, SAPH-ire, to find PTM 'hotspots' on SOD1 that have a high likelihood of affecting its biological functions. Interestingly, the top seven ranked PTM 'hotspots' were found in a small region of SOD1, between S98-K128. We focused our studies on one of the PTM 'hotspots' found in this region, lysine-122 (K122).

K122 is found in the electrostatic loop of SOD1, a loop that is important for shuttling in superoxide radicals to be neutralized. According to our data, and other studies, this lysine is both succinylated and acetylated. We found that acetyl and succinyl-mimetics (K122Q and K122E, respectively) of this site do not affect its ROS scavenging activity but do prevent SOD1 from suppressing respiration and decrease its localization to the mitochondria. Further, when cells are depleted of SIRT5 (the desuccinylase for K122), SOD1 can no longer suppress respiration. Additionally, we found that SOD1 appears to suppress respiration at complex I, whether directly or through an indirect pathway is unknown. When HCT116 colon cancer cells were depleted of endogenous SOD1, the overexpressed succinyl K122-mimetic (K122E) could not recover growth as well as overexpressed WT SOD1. The K122E SOD1 expressing cells also exhibited increased mitochondrial ROS and unhealthier mitochondria. We propose a mechanism whereby SOD1 suppression of respiration acts as an additional regulator of oxidative stress: SOD1 suppresses the electron transport chain to decrease reactive oxygen species leakage and to promote healthier mitochondria and growth.

Keywords: SOD1, post-translational modification, acetylation, succinylation, acylation, electron transport chain

ACKNOWLEDGEMENTS

First and foremost, I want to thank the person who has been my number one fan throughout this journey—my husband, Chase. He has worked toward this dissertation with me from the start by offering unconditional love, support, and encouragement. My parents deserve a huge thank you for helping me feel like I could keep going, one failed experiment after another. My siblings have also been a constant support. My Banks family has offered so much encouragement and concern. I am grateful for the fasts and countless prayers that have been offered in my behalf.

Of course, I cannot thank my advisor, Josh Andersen, enough for staying positive and having new, exciting ideas after all my negative experiments. I could not have asked for a better mentor. Everyone who has been part of the SOD1 team also deserves a huge thank you. Nathan Rodriguez played a huge role in moving the project forward and Kyle Gashler was also a big help. I am grateful for all the Andersen lab members/friends throughout the years. We have shared many laughs and they have made each day in the lab more fun as well as offered critical ideas and insights on the SOD1 project. I am grateful for my committee members and the rest of the department staff, faculty, and students that have made my time at BYU so enjoyable. The Simmons Center for Cancer Research has been a wonderful part of my time at BYU as well. I am also very grateful for everyone that helped on experiments including professors, collaborators, lab members, other graduate students, and technicians. I greatly appreciate the funding that made this project possible: from BYU, the Simmons Center for Cancer Research, and the Roland K. Robins fellowship.

Finally, I am so grateful to my Heavenly Father and Savior, Jesus Christ, for sending me comfort, ideas, and angels along the way (in the form of friends and family) to help me push through the frustrating times. This has truly been a team effort and I could not have been blessed with better friends and family as teammates along the way.

TABLE OF CONTENTS

LIST OF FIGURES

LIST OF TABLES

LIST OF ABBREVIATIONS USED

SOD1 = Superoxide Dismutase 1 or Cu/Zn Superoxide Dismutase

ALS = amyotrophic lateral sclerosis

fALS = familial ALS

sALS = sporadic ALS

PTM = post-translational modification

KAT = lysine acetyl transferase

KDAC = lysine deacetylase

ROS = reactive oxygen species

RNS = reactive nitrogen species

IMS = intermembrane space

LC-MS/MS = liquid chromatography tandem mass spectrometry

SAPH-ire = structural analysis of PTM hotspots

O_2 = molecular oxygen

H_2O_2 = hydrogen peroxide

O_2^- = superoxide radical

CCS = copper chaperone for SOD1

CytB2 = *Saccharomyces cerevisiae* cytochrome b2

ETC = electron transport chain

3-NP = 3-nitropropionic acid

Dox = doxycycline

1. CHAPTER 1: Review of Literature—Post-Translational Regulation of SOD1 and New Post-Translationally Modified Sites of Interest

1.1 Summary

SOD1 is most commonly known for its ROS scavenging activity but has more recently been implicated in a few other biological roles that provide cell homeostasis. SOD1 plays an important role in many diseases including a few neurodegenerative diseases and cancer. Many mutations in SOD1 cause destabilization and misfolding. Misfolded SOD1 has been implicated as one of the main phenotypes of amyotrophic lateral sclerosis. As one might predict, many post-translational modifications of SOD1 have a similar effect on its stability. More recent studies have focused on the effect of post-translational modifications on SOD1's cell homeostasis roles including suppressing respiration, transcription factor activity, and in preserving cytoskeleton integrity. This review provides an update on the current findings for post-translational regulation of SOD1 in its various roles and, through the computational PTM 'hotspot' finder SAPH-ire, offers additional post-translationally modified sites that are predicted to be important for SOD1 regulation and merit further study.

1.2 Introduction

The enzymatic function of Cu/Zn Superoxide Dismutase (SOD1), previously known as hemocuprein, was first characterized in 1969 in the Journal of Biological Chemistry [3]. Since that time, SOD1 has been heavily studied and become increasingly important for its essential dismutase redox function and only more recently for additional cell homeostasis biological functions. SOD1 is a homodimer that binds copper and zinc and scavenges superoxide radicals by converting them to molecular oxygen and hydrogen peroxide. SOD1 appears to be essential for cell survival as

SOD1 deletion in cultured cells causes toxic oxidative damage [4, 5]. However, only a small fraction of total SOD1 appears to be essential to maintain a healthy oxidative state in the cell because Corson et al. [6] found that after titration of SOD1 into SOD1 null yeast, only 1% of total SOD1 was essential to protect against oxidative stress. This suggests that SOD1 may have additional functions and that its biological role as a reactive oxygen species (ROS) scavenger may be more complicated than originally thought.

SOD1 has been heavily studied for its role in amyotrophic lateral sclerosis (ALS) and a few other neurodegenerative diseases [7-9]. SOD1 has more recently been shown to be overexpressed in a few different cancers as well, including lung adenocarcinoma [10], non-small-cell lung cancer [11], and 70% of primary breast cancers [12]. Further, Papa et al. [13] posit that cancer cells appear to be addicted to this enzyme because of its biological roles.

Recently, SOD1 has been implicated in a few additional roles that allow it to contribute to cell homeostasis. First, SOD1 can act as a nuclear transcription factor and regulate the expression of other antioxidant genes [14, 15]. Additionally, SOD1 has been shown to suppress respiration in yeast [16] and human cells [1] and it was recently suggested that this may be an additional antioxidant role to downregulate superoxide formation from the electron transport chain (ETC) [1]. SOD1 is also important in regulating zinc and copper homeostasis [17, 18], and in preserving cytoskeletal integrity [19, 20].

Post-translational modifications (PTMs) of SOD1 have been an important facet of studying SOD1's aggregation propensity and enzymatic activity. One phenotype associated with many familial ALS (fALS) SOD1 mutants is the propensity to aggregate. Active SOD1 is found as a homodimer and destabilization of this dimer is one of the first steps in SOD1 aggregation [21]. Through molecular dynamic simulation, Khare and Dokholyan showed that amino acids in every

region of SOD1 are important for the dimer interface [22]. Thus, while many fALS point mutations in SOD1 disrupt the dimer stability, it has been posited that PTMs of SOD1 might cause a similar disruption [21]. Indeed, PTMs of SOD1 have been shown to play a role in various neurological diseases, including ALS, Parkinson's, and Alzheimer's disease, mostly for their propensity to cause SOD1 aggregation [23-28]. Despite almost 50 years of research on SOD1, only more recently has post-translational regulation come forward as an important modulator of SOD1's other biological roles as well. This is likely due to great advancements in mass spectrometry proteomics in being able to detect post-translational modifications along with the recent discoveries of SOD1's additional functions. This review is an updated comprehensive list and discussion of the current literature on post-translational modifications and regulation of SOD1, especially in regards to its newly elucidated biological roles. Additionally, this review will discuss PTM sites that are of predicted importance by the computational PTM 'hotspot' finder, SAPH-ire, that merit future study.

1.3 SOD1 Post-Translational Modifications

Post-translational modifications play a critical role in regulating protein function and stability [29-31]. The notion that so many point mutations in SOD1 cause its destabilization and misfolding makes it an excellent candidate for being altered by PTMs as well. Many PTMs on SOD1 have already been studied for their effect on SOD1 aggregation and enzymatic activity. However, more recently these PTMs have been implicated in affecting SOD1's other biological roles as well. Here we will discuss the effect of phosphorylation, lysine modifications (acylation, ubiquitination, sumoylation, and glycation), redox modifications (oxidation, glutathionylation, and cysteinylation), and nitration on SOD1's ability to maintain cell homeostasis.

1.3.1 Phosphorylation

Phospho-signaling is an important network for maintaining cell homeostasis [32]. Multiple sites of phosphorylation have been discovered on SOD1 and a few of these sites have been implicated as important for regulating some of its biological roles, including its nuclear transcription factor and cytoskeletal preservation roles (Figure 1-1 and Table 1-1) [14, 21, 33].

The first reported phosphorylation of SOD1 was discovered by Csar et al. [34] after treatment of myeloid cells with granulocyte-stimulating factor. Although they did not identify the residue that was phosphorylated, they posited that the change in charge caused by this phosphorylation may make SOD1 more susceptible to proteolytic degradation. Decreased levels of SOD1 were observed after treatment with granulocyte-stimulating factor; thus, they suggested that this phosphorylation and corresponding degradation could be an important mechanism for activating signaling pathways that are stimulated by high ROS levels.

In human erythrocytes, two sites of phosphorylation were found on SOD1, Thr-2 and either Thr-58 or Ser-59. However, Wilcox et al. [21] did not find conclusive evidence for alteration of SOD1 enzymatic activity with phosphorylation at either of these two sites. More recently, phosphorylation at Thr-2 has been linked to a possible rescue phenotype for an fALS mutant of SOD1. Fay et al. [35] have shown that a phospho-mimetic of Thr-2, T2D, stabilizes the SOD1 dimer even when it is combined with the A4V mutation that is known to destabilize SOD1 and cause fALS.

Interestingly, Hjornevik et al. [33] were able to detect phosphorylation on SOD1 by treating primary hepatocytes with nodularin, a Ser/Thr protein phosphatase inhibitor. While they could not

decipher the specific sites phosphorylated, they found that nodularin treatment increases phosphorylation of SOD1 and decreases SOD1 colocalization with actin filaments, but does not disrupt SOD1 ROS scavenging activity. They posit that the increased phosphorylation and loss of colocalization may contribute to cytoskeletal rearrangement in the early stages of apoptotic budding after nodularin treatment, although a more detailed mechanism must be uncovered. Thus, phosphorylation may control SOD1's role in preserving the cytoskeleton.

Phosphorylation at Ser-59* (S59) and Ser-98* (S98) have been shown to regulate SOD1's nuclear transcription factor activity in yeast [14]. During times of high oxidative stress, SOD1 is translocated to the nucleus to act as a nuclear transcription factor for other oxidative stress resistance and repair genes. The nuclear translocation of SOD1 is dependent on activation of ATM/Mec1 by ROS which promotes SOD1 binding to the kinase Dun1. This kinase then phosphorylates SOD1 at S59 and S98 and promotes its translocation to the nucleus to maintain genomic stability. In fact, mutation of these serines to unphosphorylatable alanines (S59,98A) abrogates SOD1 nuclear localization during oxidative stress [14].

Leitch et al. [36] discovered another site of phosphorylation in yeast SOD1 at Ser-38. While this site is not conserved in human SOD1, in yeast, the phosphorylation is stimulated upon low oxygen conditions where SOD1 expression is downregulated or when there is a loss of CCS-dependent activation of SOD1. Interestingly, no phenotypic significance of this phospho-site has been discovered yet but Leitch et al. postulate that it may tag unfolded SOD1 for fast activation by CCS or for interactions with other binding partners.

*Some studies include the start codon in residue numbering and some do not. The asterisk indicates that the numbering of the residue from this study has been changed from the original paper to make the numbering consistent across studies (start codon not included in numbering).

Table 1-1: SOD1 phosphorylation sites. Summary of SOD1 phosphorylation sites described in this paper.

Species	Residue	Modification	Significance	Reference
human	Thr-2	phosphorylation	unknown	Wilcox, 2009
human	Thr-2	phosphorylation	phospho-mimetic stabilizes SOD1 dimer, even when combined with fALS A4V mutation	Fay, 2016
human	Thr-58	phosphorylation	unknown	Wilcox, 2009
human	Ser-59	phosphorylation	unknown	Wilcox, 2009
human	unknown	phosphorylation	may cause degradation because decreased levels of SOD1 seen	Csar, 2001
human	unknown	phosphorylation	decreased SOD1 colocalization with actin filaments, may be implicated cytoskeletal rearrangement in the early stages of apoptotic budding	Hjornevik, 2012
yeast	Ser-38	phosphorylation	phosphorylation stimulated upon low oxygen conditions, postulated that this may tag unfolded SOD1 for fast activation by CCS or for binding to other partners	Leitch, 2012
yeast	Ser-59, Ser-98	phosphorylation	phosphorylated by kinase, Dun1, which promotes SOD1 nuclear localization to maintain genomic stability	Tsang, 2014

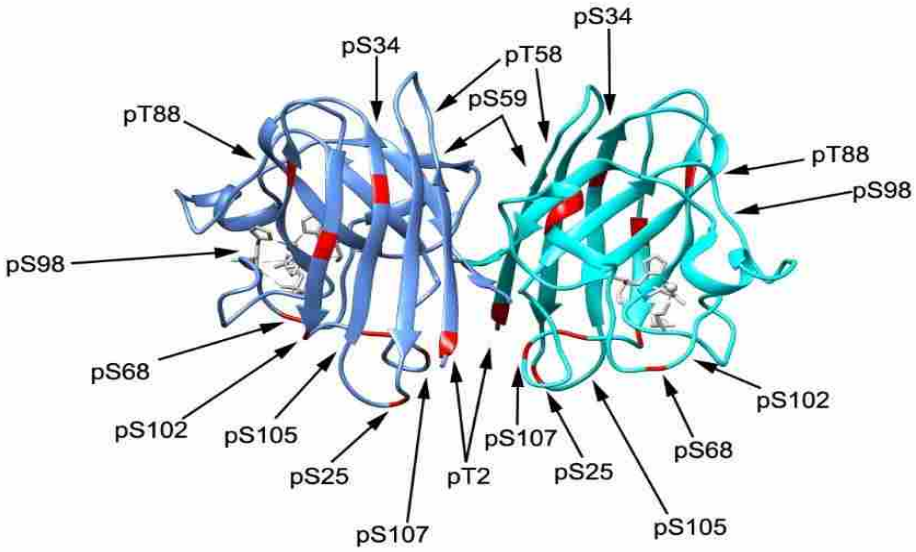

Figure 1-1. SOD1 sites of phosphorylation. Crystal structure of mouse SOD1 (PDB: 3GTV) with known human SOD1 sites of phosphorylation highlighted in red (sites compiled from papers discussed in this review and from www.phosphosite.org).

1.3.2 Lysine modifications: acylation, ubiquitination, sumoylation, glycation

Acylation. Lysine acylation is the addition of an acyl group with varying carbon chain lengths to a lysine. Lysine acylation is generally regulated by lysine acetyl transferases (KATs) and lysine deacetylases (KDACs) [37]. However, acylation can also occur non-enzymatically [38,

39]. Two types of acylation have been identified on SOD1, acetylation and succinylation, which change the net charge of a lysine from +1 to 0 and -1, respectively. These two reversible modifications frequently occur on the same lysines [40]. While many SOD1 sites of acylation have been identified through mass spectrometry, only a few have been further studied for their biological significance.

Lin et al. [41] confirmed Lys-70* (K70) as a site of acetylation in HCT116 colon cancer cells through the use of a pan-acetyl-lysine antibody. Acetylation at K70 caused inactivation of the superoxide scavenging enzymatic activity of SOD1 by disrupting binding with CCS and, in turn, decreasing the formation of SOD1 homodimers. Additionally, they identified SIRT1 as the deacetylase that regulates this site. They also demonstrated that chemotherapeutic treatment induced acetylation of SOD1. They suggested that the increase in ROS caused by chemotherapeutics caused dissociation of SOD1 and SIRT1, which increased acetylation of SOD1 and decreased its dismutase activity, further increasing ROS. Thus, SOD1 acetylation may help sensitize cancer cells to genotoxic agents.

Another acetylation site that has been highly studied for its biological significance is Lys-122* (K122), a residue found in the electrostatic loop which is the region important for shuttling in superoxide radicals [42, 43]. This site is both acetylated and succinylated [40, 44-48]. Lin et al. [49] described succinylation at this site as deactivating SOD1's enzymatic activity. However, contrary to this data, we found [1] that neither acetylation nor succinylation at K122 affect the ROS scavenging activity of SOD1 but do impair its ability to suppress respiration which, in turn, decreases its mitochondrial localization as well. Additionally, when SOD1 was knocked out of HCT116 colon cancer cells, the succinyl-mimic (K122E) of SOD1 was not able to rescue cell health as well as WT SOD1. K122E SOD1 expressing cells exhibited increased mitochondrial

ROS and lower mitochondrial membrane potential perhaps because it could not slow oxidative phosphorylation and decrease ROS leakage from the ETC. Further, these cells could not grow as quickly as cells that had WT SOD1 added back. Thus, acylation at K122 may control SOD1's ability to control oxidative health in the mitochondria by suppressing its ability to decrease respiration. We posited that this may occur through acylation disrupting binding of SOD1 to one of its interactors but this would require further study. Lin et al. [49] discovered that SIRT5 regulates desuccinylation of K122 and we found [1] that SOD1's ability to suppress respiration can be impaired by depleting cells of SIRT5.

Acetylation at K122* has also been studied in regards to the adult central nervous system. Kaliszewski et al. [44] developed an antibody specific for acetyl-K122 and used this antibody to map the regions and cell types where acetylated SOD1 at K122 was most abundant in the central nervous system. While they did not elucidate a role for acetylation at K122 in the nervous system, they did find that this acetylation was found in distinct regions and mostly restricted to a few neuronal subtypes, meriting further investigation into the biological role of SOD1 acetylation in neurons.

Although Abdolvahabi et al. [50] did not study a specific site of acetylation on SOD1, it is noteworthy to mention their study on the effect of general acetylation on the fALS phenotype of SOD1 aggregation. They found that treatment with aspirin to increase overall lysine acetylation of SOD1 could impede aggregation of A4V SOD1, a fALS-causing variant of SOD1 that is known to aggregate. Interestingly, changing the net negative charge of SOD1 by acetylation at just three lysines in the fALS-mutant A4V was enough to slow amyloidogenesis. Thus, changing the net charge of SOD1 through acetylation, or acylation in general, may prove to be an important therapeutic avenue in slowing the progression of SOD1-caused ALS.

Ubiquitination and sumoylation. Lysines are a common host for many other PTMs as well, including ubiquitination and sumoylation in the case of SOD1. Ubiquitination of a protein can target it for degradation or act as a signaling modification to alter its subcellular localization, binding to interactors, or enzymatic activity (reviewed in [51]). Sumoylation has a similar effect on proteins (reviewed in [52]).

SOD1 is modified by SUMO-1 at Lys-75. This sumoylation increases SOD1's stability and propensity to aggregate and, further, the sumoylation increases after SOD1 aggregates. Fei et al. [53] suggest that this modification may be one mechanism by which mutant SOD1 is able to accumulate and contribute toward fALS pathogenesis. There are a few sites of sumoylation in yeast SOD1, Lys-18 and Lys-69, but these lysines are not conserved in human SOD1 [54].

The PTM of ubiquitination is particularly interesting because it has primarily been connected with SOD1 as a means of degradation for the fALS mutant-SOD1 aggregates. SOD1 aggregates are degraded through two main pathways which are thought to contribute equally toward SOD1 clearance, the ubiquitin-proteasome and through macroautophagy [55]. Ubiquitin has been shown to colocalize with SOD1 aggregates in patients with fALS [56], and in G85R [57] and G93A [58] SOD1 transgenic mice. Stieber et al. [58] suggest that the increase in ubiquitin colocalization with SOD1 aggregates could be caused by a ubiquitin-proteasome pathway that cannot handle degradation of the mutant protein aggregates. Further, Basso et al. [59] suggest that the ubiquitination of SOD1 occurs after formation of the aggregates and that the ubiquitination (which branches at K48 and is the main signal for degradation) occurs at SOD1 Lys-136 but could occur at additional lysines as well. Additionally, biosensor imaging of intact single neuronal cells

Table 1-2: SOD1 lysine-modified sites. Summary of SOD1 lysine-modified sites described in this paper, including acetylation, succinylation, sumoylation, ubiquitination, and glycation.

Species	Residue	Modification	Significance	Reference
human	Lys-70	acetylation	inactivates ROS scavenging activity, deacetylated by SIRT1, may help sensitize cancer cells to genotoxic agents	Lin, 2015
human	Lys-122	succinylation	inactivates ROS scavenging activity, desuccinylated by SIRT5	Lin, 2013
human	Lys-122	acetylation/ succinylation	inhibits SOD1's anti-respiratory activity, succinyl-mimetics cause decreased growth and less healthy mitochondria in HCT116 cells, does not affect ROS scavenging activity	Banks, 2017
human	Lys-122	acetylation	acetylated SOD1 found in distinct regions of adult central nervous system	Kaliszewski, 2016
human	general	acetylation	treatment with aspirin increases SOD1 acetylation and decreases A4V SOD1 amyloidogenesis	Abdolvahabi, 2015
human	Lys-75	sumoylation	increases SOD1 stability and propensity to aggregate; sumoylation increases further after aggregation of SOD1	Fei, 2006
yeast	Lys-18, Lys-69	sumoylation	unknown	Zhou, 2004
human	Lys-136	ubiquitination	ubiquitination occurs after formation of the aggregates and may occur on additional lysines as well	Basso, 2006
human	unknown	ubiquitination	colocalizes with SOD1 aggregates in patients with fALS	Kato, 1997
human	unknown	ubiquitination	colocalizes with SOD1 aggregates in G85R and G93A SOD1 transgenic mice; Stieber et al. postulates this may be a result of the ubiquitin-proteasome pathway being unable to handle degradation of the aggregates	Bruijn, 1997; Stieber, 2000
human	unknown	ubiquitination	intact single neuronal cells demonstrated that G93A and G85R SOD1 had increased ubiquitination and colocalization with Hsp70; did not cause proteasomal dysfunction so chaperone depletion may be a cause of mutant SOD1 toxicity	Ganesan, 2008
human	Lys-3, Lys-9, Lys-30, Lys-36, Lys-122, Lys-128	glycation	Lys-122, Lys128 most critical for enzymatic deactivation	Fujii, 1996
human	unknown	glycation	does not promote amyloid formation in fALS but may cause cytotoxicity through another pathway	Sirangelo, 2016

demonstrated that mutant SOD1, G93A and G85R, have increased ubiquitination and chaperone interaction (Hsp70) over WT SOD1 but do not cause proteasomal dysfunction, which may suggest chaperone depletion and consequently decreased protein folding activity as a cause of mutant

SOD1 toxicity [60]. Inhibition of chaperone activity caused by mutant SOD1 expression has been seen previously as well [61, 62]. Dorfin, NEDL1, and MITOL have been implicated as three of the ubiquitin ligases responsible for tagging mutant SOD1 [63-65].

Glycation. Glycation of erythrocyte SOD1 has been shown to inactivate SOD1 both in vivo [66] and in vitro [67]. Interestingly, the percentage of glycated SOD1 increases in patients with diabetes [68]. In vitro, the sites of glycation were found to be Lysines 3, 9, 30, 36, 122, and 128, although glycation at Lys-122 and Lys-128 appeared to be the most critical for enzymatic deactivation of SOD1 [67]. The effect of glycation on mutant SOD1 in fALS has been reviewed in [69]. However, more recently, Sirangelo et al. [70] suggested that glycation of SOD1 does not promote amyloid formation in fALS but may cause cytotoxicity through another pathway. The known SOD1 lysine modification sites are summarized in Table 1-2 and are indicated in the SOD1 crystal structure in Figure 1-2 (human sites only).

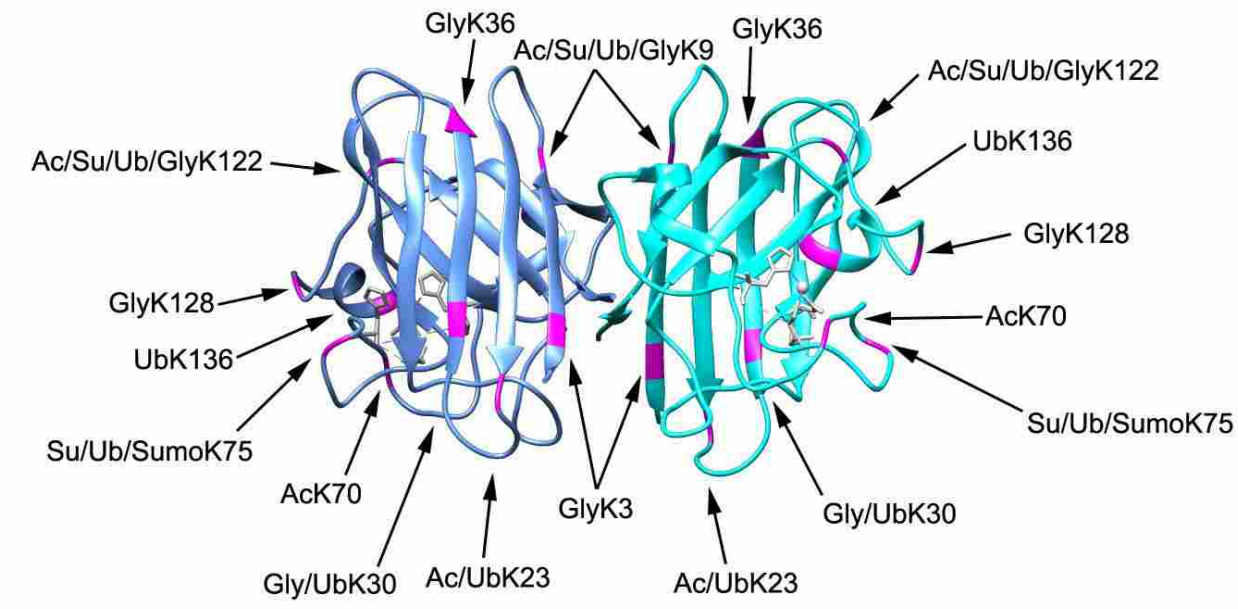

Figure 1-2. SOD1 sites of lysine modification. Crystal structure of mouse SOD1 (PDB: 3GTV) with known human SOD1 sites of lysine-modifications highlighted in magenta (sites compiled from papers discussed in this review and from www.phosphosite.org).

1.3.3 Redox modifications: oxidation, glutathionylation, and cysteinylation

Oxidation and glutathionylation. Oxidation might be one of the most interesting and influential PTMs of SOD1 to date. When wild type SOD1 is oxidized to sulfonic acid at Cys-111 it obtains similar properties to fALS mutants of SOD1—a propensity to misfold and inhibit kinesin-based fast axonal transport [71]. This draws a striking connection between fALS and sporadic forms of ALS (sALS) and may give reason for at least a subset of sALS cases. Sporadic forms of ALS are not caused by mutations in SOD1 but aggregates of WT SOD1 can still be found. Could this aggregation be caused by the PTM of oxidation? To further the idea that SOD1 oxidation may lead to sporadic forms of ALS, Martins et al. [72] used a yeast system to look for PTMs on a high molecular weight fraction of SOD1. They found that it was oxidized at C146, H71, and H120. They speculated that the increased oxidation of SOD1 leads to its misfolding and aggregation. Cys-111 appears to be a critical residue for maintaining SOD1 stability. Glutathionylation, another form of redox modifications that occur during oxidative stress, at Cys-111 destabilizes SOD1 and promotes monomer formation which is the initiating step for SOD1 aggregation [21]. Trp-32 can also be oxidized and has been shown to cause aggregation of SOD1 [73]. The sites of oxidation and glutathionylation are summarized in Table 1-3 and their positions in the SOD1 crystal structure are shown in Figure 1-3 (human sites only).

Cysteinylation. From the opposite angle but in support of the idea that oxidation may cause WT SOD1 to aggregate, cysteinylation at Cys-111 acts as a protection against oxidation of SOD1. Auclair et al. [74] found both cysteinylation and oxidation modifications on SOD1 from post-mortem human nervous tissue. Strikingly, in vitro cysteinylation offered almost full protection against peroxide-induced oxidation of other regions of SOD1. Thus, SOD1 may use cysteinylation as a defense mechanism against the destabilizing effects of oxidation. The crystal structure of

cysteinylated SOD1, while very similar to native SOD1, shows a slight conformational change at the dimer interface (loop VI) and the electrostatic loop (loop VII) [75]. Along with data collected previously for a crystal structure of 2-mercaptoethanol-modified SOD1 [76, 77] which also showed a conformational change at the electrostatic loop when Cys-111 was modified, Auclair et al. [75] predict that loops VI and VII are important for SOD1 stability. Interestingly, as we will discuss later in this paper, post-translational modifications in this region are predicted to have biological significance. Oxidation of SOD1 has proven to be a common cause of SOD1 misfolding in ALS [24-26], and thus protection from oxidative modifications by cysteinylation may be an important therapeutic avenue for future studies [75]. The cysteinylation site is shown in Figure 1-3 and summarized in Table 1-3.

Table 1-3: SOD1 redox-modified sites. Summary of SOD1 redox-modified sites described in this paper, including oxidation, glutathionylation, and cysteinylation.

Species	Residue	Modification	Significance	Reference
human	Trp-32	oxidation	increases aggregation of SOD1	Zhang, 2003
human	Cys-111	oxidation	increases SOD1 propensity to misfold and inhibit kinesin-based fast axonal transport	Bosco, 2010
yeast	Cys-146, His-71, His-120	oxidation	speculated that oxidation leads to SOD1 misfolding and aggregation	Martins, 2014
human	Cys-111	glutathionylation	destabilizes SOD1 and promotes monomer formation which is the initiating step for SOD1 aggregation	Wilcox, 2009
human	Cys-111	cysteinylation	protects SOD1 from oxidation; slight conformational change at the dimer interface and electrostatic loop	Auclair, 2013a; Auclair, 2013b

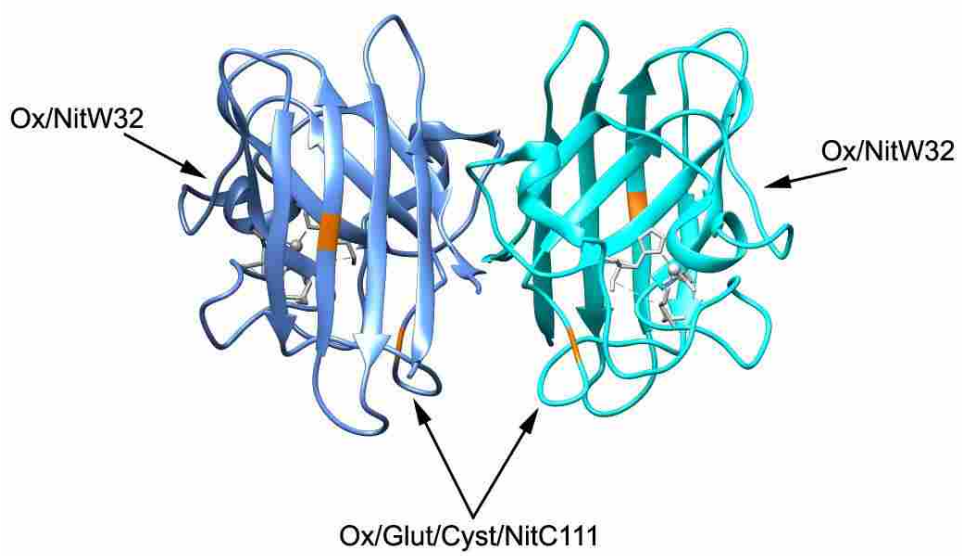

Figure 1-3. SOD1 sites of redox and nitration modifications. Crystal structure of mouse SOD1 (PDB: 3GTV) with known human SOD1 sites of redox and nitration modifications highlighted in orange (sites compiled from papers discussed in this review).

1.3.4 Nitration

Similar to ROS, reactive nitrogen species (RNS) can also play a role in causing diseases [78-80]. Nitration modifications occur when a protein reacts with a RNS. Nitration of SOD1 has been reviewed in [81]. In brief, bovine SOD1 has been shown to contain 3-nitrotyrosine residues after reaction with peroxynitrite (a reactive nitrogen species) but the modified enzyme did not have a reduction in dismutase activity [82]. Human SOD1 does not contain any tyrosine residues but can still be nitrated at Trp-32 to 6-nitrotryptophan which demonstrates a partial loss of dismutase activity [83, 84]. In another study, peroxynitrite reaction with human SOD1 led to inactivation of its enzymatic activity but also histidinyl radical formation [85]. Further, substitution of Trp-32 with a phenylalanine decreased the cytotoxicity and aggregation propensity of a fALS mutant of SOD1 [86]. As mentioned earlier, Trp-32 can also be oxidized and has been shown to cause aggregation of SOD1 [73]. The known SOD1 nitration sites are shown in Figure 1-3 (human sites only) and summarized in Table 1-4.

Table 1-4: SOD1 nitration sites. Summary of SOD1 nitration sites described in this paper.

Species	Residue	Modification	Significance	Reference
human	Trp-32	nitration	partial loss of dismutase activity	Yamakura, 2001; Yamakura, 2005
human	Trp-32		substitution of Trp-32 with Phenylalanine decreases cytotoxicity and aggregation propensity of fALS mutant of SOD1	Taylor, 2007
bovine	unknown	nitration	no effect on dismutase activity	Ischiropoulos, 1992

1.4 SAPH-ire Data

To facilitate future studies on PTM-regulation of SOD1, we used the tool SAPH-ire to predict which domains and residues on SOD1 would most likely contain biologically relevant PTMs [1]. SAPH-ire is a computational tool that compares protein domains and their experimentally-identified post-translational modifications and predicts which PTMs might affect biological function of the protein of interest [87-89]. SAPH-ire gives each modified amino acid a FPx score that correlates with its likelihood of being biologically significant. When comparing SOD-like domains, we found a small region of SOD1 that contained seven residues with the highest FPx scores (highlighted in Figure 1-4; described in more detail in [1]). It is striking that the top seven scores were found in this region of only 30 amino acids between Ser-98 and Lys-128.

Further, this region contains part of the dimer interface (loop VI; residues 102-115) [77] and the electrostatic loop (loop VII; residues 122-143) [90]. Interestingly, loop VI encompasses Cys-111 which as discussed earlier is extremely important in preserving the dimer interface and SOD1 stability [74, 75]. Destabilization of the dimer interface and the electrostatic loop have been implicated in fALS [25, 91-94]. Small disturbances in the structure of this region may prove crucial for altering SOD1 function and stability [75]. Only a few of the top seven FPx scored-amino acids have been studied for their biological significance and future studies will need to be conducted regarding the rest of the PTMs in this region, namely the PTMs at Ser-102, Ser-105, Ser-107, Ser-

111, Lys-122, and Lys-128. The residues in this region are shown with their FPx rank in Table 1-5 along with what is currently known about each PTM.

Table 1-5: Highest ranked SAPH-ire PTM sites. The highest ranked SAPH-ire PTM sites along with the predominant PTMs identified and what is known about these PTMs from the literature. Table adapted from [1].

SAPH-ire FPx RANK	MAP ID (IPR001424)	Residue in Mouse (P08228)	Predominant PTM	SAPH-ire Score (rel to max)	What is Already Known about this PTM	Reference
1	129	S-98	Phos.	100	phosphorylation promotes SOD1 nuclear localization to maintain genomic stability; kinase is Dun1	Tsang, 2014
2	142	S-111	Phos.	35		
3	138	S-107	Phos.	24		
4	167	K-128	Ac./Ub./Gly.	19	glycation causes enzymatic deactivation	Fujii, 1996
5	133	R-102 (human S-102)	Phos.	18		
6	155	K-122	Ac./Su./Ub./Gly.	16	succinylation inactivates ROS scavenging activity; desuccinylated by SIRT5	Lin, 2013
					acetylation/succinylation inhibit SOD1's anti-respiratory activity, succinyl-mimetics cause decreased growth and less healthy mitochondria in HCT116 cells, does not affect ROS scavenging activity	Banks, in press
					acetylated SOD1 found in distinct regions of adult central nervous system	Kaliszewski, 2016
7	136	S-105	Phos.	14		

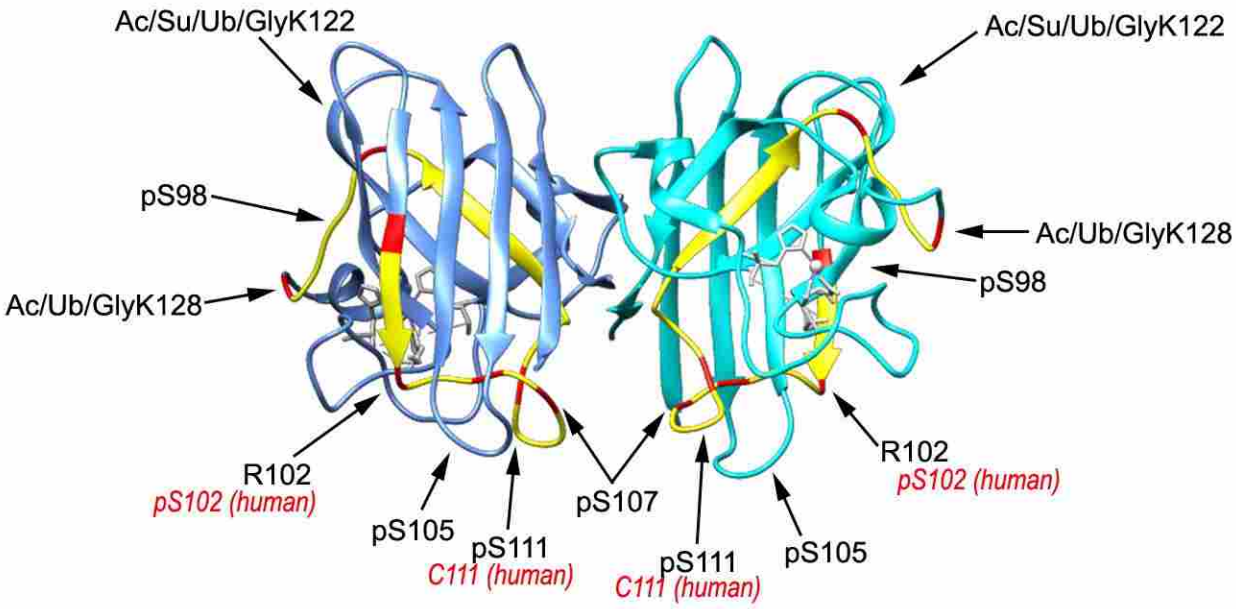

Figure 1-4. Highest ranked PTM 'hotspots' identified by SAPH-ire. Crystal structure of mouse SOD1 (PDB: 3GTV) with highest ranked PTM hotspots identified by SAPH-ire highlighted in red and the region between S98-K128 (which contains the seven highest ranked PTM hotspots) highlighted in yellow. Residues labeled in black are the mouse sites with the corresponding human site labeled in red. Figure adapted from [1].

1.5 Discussion

SOD1 has long been a subject of interest for its connection to ALS. For being comprised of only 154 amino acids, it is surprising that over 160 mutations in *SOD1* have been found in patients with ALS. Further, at least 75 of the 154 amino acids have been found to contain point mutations in the *SOD1* gene of patients with ALS [95]. Many of these mutations cause destabilization and misfolding of the protein, leading to its aggregation and amyloidogenesis. Thus, it is not surprising that PTMs on SOD1 have been studied for their effect on SOD1 destabilization and aggregation propensity [23-28]. In more recent years, SOD1 has been highlighted for new biological roles aside from its ROS scavenging activity. These findings along with improvements in mass spectrometry have allowed many researchers to begin discovering how PTMs regulate SOD1's newly discovered biological roles. For example, phosphorylation at Ser-59 and Ser-98 in yeast causes SOD1 to translocate to the nucleus and act as a transcription factor

for other genes that regulate oxidative stress [14]. Acylation at Lys-122 has been shown to regulate SOD1's ability to suppress respiration [1]. Identifying and studying the effect of post-translational modifications on SOD1 will continue to expand our understanding of this complex protein that is ubiquitous and highly expressed.

We used the computational analysis tool, SAPH-ire, to hone in on important regions of SOD1 for PTM regulation. SAPH-ire predicts PTM 'hotspots' that are most likely to affect biological function of a protein. Interestingly, for SOD1, the top seven predicted 'hotspots' were in a small region of SOD1 of only 30 amino acids, between Ser-98 and Lys-128 [1]. This region is particularly interesting because it contains part of the dimer interface, Cys-111, and the electrostatic loop—which have all been implicated in maintaining SOD1 stability [25, 74, 75, 77, 90-94]. A few of the sites in this region have already been studied for their PTM-regulation but many of them will be important candidates for helping us understand the regulation of SOD1's various and diverse biological roles.

2. CHAPTER 2: Acylation of Superoxide Dismutase 1 (SOD1) at K122 Governs SOD1-mediated Inhibition of Mitochondrial Respiration

*This chapter is currently *in press* with minor variations from this version:
Banks, C.J., Rodriguez, N.W., Gashler, K.R., Pandya, R., Mortenson, J.B., Whited, M.D., Soderblom, E.J., Thompson, J.W., Moseley, M.A., Reddi, A.R., Tessem, J.S., Torres, M.P., Bikman, B.T. & Andersen, J.L., *Acylation of Superoxide Dismutase 1 (SOD1) at K122 Governs SOD1-mediated Inhibition of Mitochondrial Respiration.* Molecular and Cellular Biology, In Press.

2.1 Summary

Here we employed proteomics to identify mechanisms of post-translational regulation on cell survival signaling proteins. We focused on Cu/Zn Superoxide Dismutase (SOD1), which protects cells from oxidative stress. We found that acylation of K122 on SOD1, while not impacting SOD1 catalytic activity, suppressed the ability of SOD1 to inhibit mitochondrial metabolism at respiratory complex I. We found that deacylase depletion increased K122 acylation on SOD1, which blocked suppression of respiration in a K122-dependent manner. In addition, we found that acyl-mimicking mutations at K122 decreased SOD1 accumulation in mitochondria, initially hinting that SOD1 may inhibit respiration directly within the intermembrane space (IMS). However, surprisingly, we found that forcing the K122 acyl mutants into the mitochondria with an IMS-targeting tag did not recover their ability to suppress respiration. Moreover, we found that suppressing or boosting respiration levels toggled SOD1 in or out of the mitochondria, respectively. These findings place SOD1-mediated inhibition of respiration upstream of its mitochondrial localization. Lastly, deletion-rescue experiments show that a respiration-defective mutant of SOD1 is also impaired in its ability to rescue cells from toxicity caused by SOD1 deletion. Together, these data suggest a new interplay between SOD1 acylation, metabolic regulation, and SOD1-mediated cell survival.

2.2 Introduction

The regulation of cell signaling events through protein post-translational modifications (PTMs), including phosphorylation, acylation, glycosylation and ubiquitination, provides a means for cells to respond rapidly to environmental cues. Defects in the pathways that control PTMs underlie many human diseases and typically represent a fundamental breakdown in communication between the cell and its environment. Mass spectrometry-based approaches have dramatically expanded our view of PTMs, both in terms of PTM variety and proteome coverage. Over 200 different PTMs have been described (uniprot.org) and many, including phosphorylation and ubiquitination, regulate essentially every known biological process in the cell. With this understanding of PTM breadth, the challenge is to now 'zoom in' to understand the functional consequences of specific PTMs. Thus, our goal is to understand how PTMs affect protein function, with particular focus on cell survival signaling nodes and pathways.

Here we used an affinity purification approach, coupled with liquid chromatography tandem mass spectrometry (LC-MS/MS), to identify PTMs in primary untreated mouse tissues. Using a recently developed PTM analysis tool (SAPH-ire) to prioritize our functional studies, we evaluated PTMs from our experiment against all other experimentally observed PTMs curated for the Cu/Zn Superoxide Dismutase (SOD) domain family [87, 89]. This analysis highlighted an acyl-modified lysine on SOD1, which we focused on in this study. SOD1 is a well conserved metalloenzyme best known for its catalytic role in disproportionation of superoxide radicals (O_2^-) into molecular oxygen (O_2) and hydrogen peroxide (H_2O_2) [3, 17, 96-102]. Its expression is primarily cytosolic, although a fraction of SOD1 exists in the mitochondrial intermembrane space (IMS). Studies spanning multiple model organisms and cell lines have underscored the importance of SOD1 in oxidative stress protection (reviewed in [103, 104]). Accordingly, SOD1 is overexpressed in a variety of cancers and SOD1 deletion in mice results in a higher incidence of

liver cancer [98]. Additionally, mutations in SOD1 that increase its propensity to aggregate cause toxicity in motor neurons, resulting in a familial form of amyotrophic lateral sclerosis (ALS) (reviewed in [104]).

Several lines of evidence suggest that SOD1 biology may be more complex than initially thought. While SOD1 deletion is toxic in cultured cells due to an accumulation of oxidative damage [4, 5], titration of SOD1 expression against a SOD1 null background in yeast revealed that only a small fraction, representing about 1% of total SOD1, is required for protection against oxidative stress [105]. This suggests that SOD1 may have additional functions beyond its traditional role in reactive oxygen species (ROS) scavenging. Indeed, studies suggest that SOD1 has roles in zinc and copper buffering [17, 18] and in regulating gene transcription [14, 15]. In addition, a recent study by Reddi and Culotta found that yeast SOD1 suppressed mitochondrial respiration [16]. However, despite this emerging complexity in SOD1 biology and clear roles for SOD1 in human disease, we have a limited understanding of SOD1 regulation at a post-translational level.

Here we uncover a novel regulatory mechanism by which a Sirtuin-governed acylation within the electrostatic loop of SOD1, at K122, suppresses SOD1-mediated inhibition of mitochondrial metabolism in mammalian cells. This observation provided genetic tools to help understand the relationship between SOD1 mitochondrial localization and metabolic regulation as well as the potential contribution of this SOD1 metabolic function to its role in promoting cell survival. Our data suggest a model in which Sirtuin-mediated deacylation of SOD1 promotes its inhibition of respiration, which in turn, elevates levels of mitochondrial SOD1 and contributes to SOD1's pro-survival function.

2.3 Materials and Methods

2.3.1 Mass Spectrometry and PTM Affinity Purifications. Trypsin-digested cell lysates from mouse embryo, brain, and liver were prepared by lysis in 8 M urea, followed by normalization to approximately 2 mg/mL and 1.8 M Urea, reduced with 10 mM dithiothreitol, alkylated with 20 mM iodoacetamide, and digested with TPCK trypsin at 1:25 w/w. Peptides were desalted with C18 SPE cartridges (Waters) and lyophilized to dryness. Approximately 5 mg aliquots of each lysate digest was enriched for post-translational modifications using the PTMScan product line (Cell Signaling Technologies), including a series of phospho-specific motifs (AKT, MAPK, phosphothreonine, or pY) as well as ubiquitin remnant (GG-K), or acetyl-lysine (Kac), as previously described [106-108]. Titanium dioxide enrichment was performed as previously described, for comparison [108].

After immunoaffinity or titanium dioxide enrichment, peptides were analyzed using data-dependent acquisition (DDA) by a 3-fraction LC/LC-MS/MS method as previously described [109]. Samples were resuspended in 12 µl of 1/2/97 v/v/v TFA/MeCN/water. Phosphopeptide samples additionally contained 20 mM citric acid. Approximately half of each sample was analyzed on a 2D nanoAcquity UPLC coupled to a Synapt G2 HDMS (Waters Corporation). Searchable files (*.mgf) were generated from raw data in Mascot Distiller, and database searching for peptide ID and Mascot search engine v2.4 (Matrix Science, Inc.). The UniProt database (www.uniprot.org) with *mus musculus* taxonomy and reviewed status was utilized, along with 10 ppm precursor and 0.04 Da product ions. Fixed modification of Cys with carbamidomethylation was required, and variable modifications included deamidation NQ, oxidation M, along with acetylated K, ubiquitin remnant, or phosphorylated S/T/Y. Full tryptic specificity was required. Data was curated in Scaffold v4.7 using PeptideProphet algorithm, to a 0.05% peptide and 0.4% protein FDR. The Scaffold file is available for download at https://discovery.genome.duke.edu

/express/resources/3023/3023_PTMScanAll_withTiO2.sf3. All mouse experiments were IACUC approved.

2.3.2 SAPH-ire. SAPH-ire FPx was employed as described previously [89], with modifications for the domain-specific analysis of the superoxide dismutase (SOD) copper/zinc binding domain (IPR001424). FPx scores were calculated using the structure-free 8-factor neural network model as described previously [87]. The SOD domain sequences for all eukaryotic proteins were obtained from Pfam [110]. The multi-FASTA files generated for the domain family were subsequently aligned using MUSCLE with default parameters [111]. The domain dataset for SOD contained 79 unique sequences within which 77 distinct PTMs could be retrieved from the public domain. PTMs coalesced into 34 modified alignment positions (MAPs) in the family, the features of which were used for SAPH-ire FPx scoring.

2.3.3 Cell Culture and Reagents. HEK293T cells were purchased from ATCC. Flp-In T-REx 293 host cell line was purchased from Thermo Fisher Scientific (R78007). The Flp-In T-REx HCT-116 host cells were developed by Dr. Stephen Taylor [112]. All cell lines were cultured in Dulbecco's modified Eagle's medium (DMEM, Gibco no. 11965) supplemented with 10% fetal bovine serum (FBS) at 37 ºC in a 5% CO_2 incubator.

Antimycin A (A8674), 3-Nitropropionic acid (3-NP) (N5636), galactose (G5388), tetracycline (T7660), and doxycycline (D3447) were purchased from Sigma. Rotenone was purchased from Millipore (557368). Drugs used in cell culture were dissolved in the recommended solvent and then diluted in cell culture media to the indicated final concentrations.

2.3.4 Plasmid Transfections and siRNA. Cells were transfected with plasmid expression vectors pcDNA3.1, HA- or FLAG-SOD1 with polyethylenimine (PEI, Polyscience Inc.) transfection reagent in a 1:3-4 (µg DNA:mg PEI) ratio. Site-directed mutants of FLAG-SOD1

were generated using the Agilent QuikChange II XL kit (200521) or the Q5 Site Directed Mutagenesis kit from New England Biolabs, Inc. (E0554). Plasmids and selection reagents for Flp-In T-REx host cell lines were obtained from Thermo Fisher Scientific. RNAiMAX Lipofectamine reagent was purchased from Invitrogen (13778100). Smartpool siRNA against SIRT5 was obtained from GE Dharmacon (M013448010005). The Cytochrome B2 SOD1 cDNA was obtained from Dr. Giovanni Manfredi.

2.3.5 Generation of Flp-In T-REx Cell Lines. Generation of T-REx cells lines with Flp-recombinase mediated gene insertion allows for tight control of expression of a gene of interest at a single, actively transcribed genomic locus by addition or removal of tetracycline or its derivatives. For further explanation, refer to the manufacturer's manual (Thermo Fisher Scientific no. R78007).

T-REx host cells were transiently transfected with pOG44 and pcDNA5/FRT/TO-FLAG-SOD1, including WT SOD1 and acyl-mimicking mutants, at a ratio of 9:1 (pOG44:pcDNA5). Constructs were co-transfected into cells in 6-well plates when cells were approximately 60% confluent. After 48 hours, cells were trypsinized and transferred to 15 cm cell culture dishes and cultured in complete medium containing 150 μg/mL of hygromycin B selection reagent (Gibco 10687010). After 10 days, single colonies were transferred to individual wells of a 24-well plate and cultured in medium without selection reagent. Plates were replicated and expression was induced for 24 hours with 1 μg/mL tetracycline in one set of the replicates, after which cells were harvested, lysed, and subjected to Western blot analysis as described below. Cells positive for the FLAG epitope were selected, and cells with the lowest background expression when not induced, but still exhibiting high inducible expression with tetracycline, were selected

for use in experiments. For experiments, expression was induced with either tetracycline or doxycycline at a final concentration of 100 ng/mL.

2.3.6 Antibodies. Primary mouse monoclonal anti-HA (7392), rabbit polyclonal anti-FLAG (807), mouse monoclonal and rabbit polyclonal anti-beta actin (8432, 1616) were purchased from Santa Cruz Biotechnology. Primary mouse monoclonal anti-FLAG (8146), rabbit polyclonal anti-FLAG (2368), mouse monoclonal and rabbit polyclonal anti-human SOD1 (4266, 2770), mouse monoclonal anti-HA (2367), rabbit monoclonal anti-SIRT5 (8779), and rabbit polyclonal anti-VDAC (4661) were purchased from Cell Signaling Technology, Inc. Primary mouse monoclonal anti-GAPDH and rabbit monoclonal anti-MEK1/2 were purchased from Abcam (9484, 178876). Anti-mouse and anti-rabbit IRDye 680RD and IRDye 800CW secondary antibodies were purchased from Licor (92668070, 92632210, 92668071, and 92632213).

Succinyl-Lys122 Antibody Purification: Rabbits were immunized against the succinylated-SOD1 peptide (LVVHE[succinyl-K]ADDLGC) and serum was collected. Succinyl-Lys122 polyclonal antibody was immunopurified out of serum using succinylated Lys122 SOD1 peptide as previously reported [113]. In brief, biotinylated (non-succinyl) Lys122 peptide was conjugated to streptavidin-agarose (20359, Thermo Scientific) and gently rotated at 4 ºC overnight with rabbit serum diluted 1:1 in equilibration buffer (150 mM Tris [pH 7.5], 20 mM NaCl) to deplete non-succinyl Lys122-specific antibody from serum. Following incubation, serum was transferred to a column containing succinylated Lys122 peptide conjugated to streptavidin resin and again incubated overnight with gentle rotating. Resin was thereafter washed twice with equilibration buffer. Succinyl Lys122-specific antibody was then eluted from resin with elution buffer (0.1 M glycine-HCl [pH 2.8]) by gravity elution. Fractions were then collected in microfuge tubes and

neutralized with neutralization buffer (1 M Tris-HCl [pH 8.5]). Reactivity of each fraction was tested via Western blot for antibody titer.

Primary anti-human SOD1 succinyl-Lys122 antibody serum, biotinylated SOD1 succinyl-Lys122 peptide, and biotinylated SOD1 non-succinyl Lys122 peptide were produced by Eton Bioscience, Inc.

2.3.7 Western Blotting and Immunoprecipitation. Cells were seeded in 10 cm or 6-well plates to 15% confluence. After 24 hours, at about 30% confluence, T-REx cells were induced, or non T-REx cells were transfected with a SOD1 expression vector, an empty vector, or mock transfected. After 8 hours, cell culture medium was replaced with complete medium and incubated at 37 ºC in a cell culture incubator until 48 hours post-transfection. Cells receiving drug treatment were treated within this incubation time at the indicated concentrations. Cells treated with RNA interference were transfected with 100 nM SIRT5-directed or scrambled siRNA with RNAiMAX Lipofectamine. The knock-down was repeated to ensure efficient depletion of SIRT5. Then cells were allowed to grow 24 to 48 more hours. Following transfection and incubation, cells were washed twice and harvested with ice-cold PBS. Cells were then lysed in ice-cold coimmunoprecipitation buffer (10 mM HEPES [pH 7.5], 150 mM KCl, 0.1% NP-40) or TNTE coimmunoprecipitation buffer (20 mM Tris [pH 7.8], 150 mM NaCl, 0.3% w/v triton X-100, 5mM EDTA), supplemented with protease inhibitors (88665 Pierce). Lysates were then cleared by centrifugation at 21,000 x g for 10 minutes at 4 ºC. Lysate protein concentration was determined by a Bio-Rad protein determination DC Assay (5000116). Lysate was saved for analysis or incubated with 15 µL of anti-FLAG-agarose resin (2220 Sigma). Protein was eluted from the resin by incubation with modified Laemmli buffer for 5 minutes at 100 ºC. Lysates were likewise mixed and boiled in modified Laemmli buffer. Samples were then loaded onto SDS PAGE gels. Bluestain

protein ladder (P007 GoldBio) was used as a molecular weight reference. Gels were then transferred to a PVDF membrane and immunoblotted for proteins of interest. Proteins were visualized and bands were quantified using the LI-COR Odyssey Classic or CLx imaging systems and Image Studio software package.

2.3.8 SOD1 Activity Assays. For the *in vitro* colorimetric activity assay, HEK293T cells were transfected with a FLAG-SOD1 plasmid or mock transfected. Cells were harvested, lysed, and FLAG was immunoprecipitated with FLAG epitope-conjugated agarose beads, after which the resin was washed 3x in cold PBS. FLAG-SOD1 was then competitively eluted from the beads by incubation in a 200 ng/µL solution of purified FLAG peptide (Apex Bio), with gentle shaking for 10 minutes at 4 ºC. Beads were then centrifuged at 8,200 x g for 30 seconds at 4 ºC. The FLAG-SOD1-containing supernatant was transferred to a new microfuge tube and the elution was repeated and added to the same tube. With the purified SOD1 or mock supernatants, SOD1 ROS scavenging activity was indirectly measured using a SOD Assay Kit purchased from Sigma (19160), according to manufacturer's recommendations.

For the *in situ* SOD1 activity gel, purified FLAG-SOD1 was produced as in the colorimetric assay. SOD1 ROS scavenging activity was indirectly measured as a competitive reaction of superoxide with nitroblue tetrazolium (NBT) dye as previously described [114]. Briefly, a portion of the purified SOD1 supernatants were mixed with 5x SOD loading dye (25 mM Tris-HCl [pH6.8], 50% glycerol, 0.5% bromophenol blue) to a final concentration of 1x loading dye. Samples were then loaded onto an 8% native PAGE gel and SOD1 was resolved at 80 V constant until the loading dye reached the end of the gel. The gel apparatus was maintained at 4 ºC. The gel was then moved to a shallow container, immersed in 50 mL of staining solution (45 mM K_2HPO_4, 4.6 mM KH_2PO_4, 0.163 mM NBT, 0.266 mM riboflavin), and covered with foil.

50 µL of TEMED was then added and the gel was incubated with gentle shaking for 1 hour in the dark. Following incubation, the staining solution was removed and the gel was washed 2x with distilled water, and then immersed and incubated in distilled water with gentle shaking overnight, while exposed to ambient light. Clear bands on the blue-stained gel were interpreted as active SOD1. NBT (N6639), K_2HPO_4 (P3786), KH_2PO_4 (P0662), and riboflavin (R9504) were purchased from Sigma.

2.3.9 Cell Survival Assay. Single-guide RNA (sgRNA) against SOD1 was cloned into the pSpCas9(BB)-2A-Puro (PX459) vector. PX459 was a gift from Feng Zhang (Addgene plasmid # 48139) [115]. Human codon–optimized Cas9 from S. *pyogenes* and the sgRNA were expressed from the human cytomegalovirus (CMV) immediate early promoter and the human U6 promoter, respectively. The SOD1-targeted 20 base pair sgRNA contained the sequence TTGCATCATTGGCCGCACAC with an NGG protospacer adjacent motif (PAM) site of TGG. Knock-out efficiency was measured via Western blot analysis. The construct was transfected into T-REx HCT-116 cells. After eight hours, transfection medium was removed and replaced with DMEM complete medium. 24 hours post-transfection, cell culture medium was replaced with DMEM complete medium containing 3 µg/mL puromycin selection reagent. After 48 hours, selection medium was removed and replaced with DMEM complete medium containing 100 ng/mL doxycycline. Doxycycline medium was replenished every 48 hours and cells were trypsinized as needed. Cells were allowed to grow until there were sufficient cells for the assays, after which cells were trypsinized and counted.

Growth Assay with Giemsa Stain: For Giemsa staining, 22,500 cells per well were seeded into 6-well plates with 100 ng/mL doxycycline and allowed to grow for 5 days. Cells were then washed twice with ice cold PBS, fixed for 30 minutes in ice cold methanol at 4 ºC, after which

methanol was aspirated and a 1:20 mixture of Giemsa stain (Fluka Analytical 48900) to PBS was added to cells and incubated at room temperature for 45 minutes. Following staining, cells were washed 3 times with distilled water and allowed to air dry. Wells were imaged and quantified using the LI-COR Odyssey Classic imaging system and Image Studio software package.

Incucyte Zoom Analysis: For Incucyte analysis of control cells without SOD1 knockout, 12,500 cells were seeded per well into 12-well plates. For the SOD1 knockout/addback cells 18,000 cells were seeded per well into 24-well plates. Plates were put into the Incucyte one day after seeding and cell confluence was monitored via basic phase contrast analysis for 80 to 120 hours. Cell confluence was given as the mean of 4 wells per sample, 16 images per well. Error bars are represented as +/- SEM.

2.3.10 Cellular Respiration. HEK293T cells were transiently transfected with 8 μg of a SOD1 plasmid, empty pcDNA3.1, or mock transfected. Eight hours later, cell culture medium was replenished and cells were allowed to grow for a total of 48 hours. For rotenone treatment, 1 nM rotenone or vehicle was added to HEK 293 cells 30 minutes prior to measuring oxygen consumption rates, and incubated at 37 ºC in 5% CO_2 atmosphere. Cells were then detached in culture dishes with 0.05 % trypsin–EDTA (Gibco) and growth medium was added to the culture. Contents were transferred to a 15 mL conical tube and centrifuged at room temperature. After removal of supernatant, the cells were permeabilized, prepared for the Oroboros O2K (Oroboros Instruments, Innsbruck, Austria), and O_2 flux was measured as previously described by Hodson et al. [116] with the exception of a few changes as outlined below. The data presented is taken from maximal O_2 flux measurements when the full electron transport system capacity of oxidative phosphorylation was measured after addition of FCCP. For the complex I and complex II inhibition assay, rotenone (2 mM) and malonate (2.5 mM) were added prior to O_2 flux measurements. After

respiration was measured, cellular protein concentrations from the same cells were determined as in 'Western Blotting and Immunoprecipitation'. For the rotenone treated cells, 2 million cells were counted and assayed in the Oroboros O2K.

2.3.11 Endogenous Immunoprecipitation. Endogenous immunoprecipitation of SOD1 was performed using the Dynabeads Co-Immunoprecipitation Kit purchased from Thermo Fisher Scientific (14321D) according to the manufacturer's recommendations. To pull down SOD1, 7.5 mg of magnetic epoxy beads were conjugated to 37.5 µL of SOD1 antibody, per sample. As an IgG control for SOD1 immunoprecipitation, primary anti-Chk1 was conjugated to magnetic beads.

2.3.12 Mitochondrial Enrichment. All mitochondrial isolations were done with the Mitochondria Isolation Kit for Cultured Cells, obtained from Thermo Scientific (89874). Mitochondrial pellets were isolated according to manufacturer's protocol.

2.3.13 SOD1 Aggregation Assay. T-REx HEK293 with WT, G93A, or G93A/K122E SOD1 cells were plated at 20% confluence in two 15 cm plates per sample. Tetracycline was added to culture medium to induce expression of the SOD1 constructs, and cells were allowed to express for 48 hours. Tetracycline-containing medium was replenished after 24 hours due to tetracycline instability. Cells were washed twice with ice-cold PBS, removed from the plate with a cell scraper, and cells from each set of two 15 cm plates were combined (i.e., cells from the two WT-SOD1 plates were combined, etc.) to a total of three samples. Cells were lysed in 600 µL of TNTE coimmunoprecipitation buffer containing protease inhibitors by gentle rotation at 4 °C for 25 minutes. Following incubation, cells were passaged 10 times through a 25-G needle. Lysates were cleared by centrifugation at 21,000 x g for 10 minutes at 4 °C. Five-hundred microliters of lysate were loaded onto a Superdex 200 10/300 GL size exclusion column and separated and eluted with PBS on an AKTA-Pure FPLC system (GE Healthcare). Lysates were fractionated at a rate of 0.5

mL/min into 48 fractions. Fractions were resolved via SDS PAGE on a 15% gel and immunostained for FLAG and endogenous SOD1.

2.3.14 Mitochondrial Membrane Potential Assay. Mitochondrial membrane potential in cells (same cells as in the Cell Survival Assay, described above) was assayed with the JC-1 Mitochondrial Membrane Potential Assay Kit (Abcam 113850) based on an adaptation of the manufacturer's instructions. Specifically, for each sample, medium was collected and saved in a 12x75 mm polystyrene test tube. Cells were washed once with PBS, which was added to the corresponding test tube. Following the wash, cells were trypsinized and cells were collected into the same tube. Tubes were capped and centrifuged at 1000 x g for 5 minutes. The supernatant was discarded and cells were resuspended in 1 mL of warm complete medium. 10 µL of 200 µM JC-1 in DMSO was then added to each sample. No stain was added to a separate sample, as a control. After addition of stain, the samples were protected from light and incubated at 37 ºC for 20 minutes, followed by a single 2 mL wash with PBS. Cells were resuspended in 500 µL of PBS and analyzed on an Accuri C6 flow cytometer. Emission spectra from excitation at 488 nm were detected with the FL-1 and FL-2 emission filters. Standard compensation was carried out based on control Cas9 cells.

2.3.15 Mitochondrial ROS Determination. The relative number of high ROS containing cells (same cells as in the Cell Survival Assay) was determined by a flow cytometry-based application of MitoSOX Red Mitochondrial Superoxide Indicator (Life Technologies M36008). After cells were grown to 80% confluence in 12-well plates, 10 mM antimycin A was added to the positive control cells to a final concentration of 30 µM and incubated for 40 minutes in a 5% CO_2, 37 ºC incubator. Following incubation, cell medium was collected and saved in a 12x75 mm polystyrene test tube. Cells were washed once with PBS, which was added to the corresponding

test tube. Following the wash, cells were trypsinized and cells were collected into the same tube. Tubes were capped and centrifuged at 600 x g for 3 minutes. The supernatant was discarded and cells were washed once in 1 mL of warm complete medium. To stain cells, 5 mM MitoSOX Red was prepared in DMSO as indicated by the manufacturer, which was then diluted to 5 μM in complete medium. All samples were resuspended in 1 mL of the 5 μM MitoSOX-containing medium, except the negative control which was resuspended in 1 mL of complete medium. After addition of stain, the samples were protected from light and incubated for 10 minutes at 37 ºC and 5% CO_2, followed by a 3-minute centrifugation at 600 x g and a single 1 mL PBS wash. Cells were resuspended in 1 mL of PBS and passed through a 70 μm cell strainer, diluted to approximately 500,000 cells/mL, and analyzed on either an Accuri C6 or an Attune Acoustic Focusing Cytometer (Life Technologies). Emission spectra from excitation at 488 nm were detected with the BL-3 or FL-3 emission filter.

2.3.16 Live Cell Confocal Imaging. Cells (same as in the Cell Survival Assay) were seeded at medium density into 35 mm glass bottom microwell dishes (MatTek, P35GC-1.5-10-C) and allowed to adhere for 24 hours. Prior to staining, positive control cells were treated for 40 minutes with 30 μM antimycin A. To stain cells, MitoSOX Red was prepared as in the ROS determination assay, cells were washed once with warm complete medium, and 1 mL of MitoSOX medium was added to each plate, except the negative control (1 mL complete medium). Cells were incubated protected from light for 10 minutes at 37 ºC and 5% CO_2 atmosphere, after which they were washed 3 x with warm complete medium. Nuclei were counterstained with 1 μg/mL Hoechst 33342 (Pierce 62249) according to manufacturer's protocol, using a 10-minute incubation time, followed by a PBS wash. Cells were then treated for at least 45 minutes with 1 mL of ProLong Live Antifade Reagent, for live cell imaging (Molecular Probes P36975), 1:100 in complete

DMEM. Finally, at the time of imaging the plate was transferred to a humidified, 5% CO_2, 37 ºC mini chamber adapted to the microscope stage.

Cells were imaged on a Leica (Buffalo Grove, IL, USA) TCS SP8 HyD using the resonance scanning mode. Images were collected from a 63x oil objective. Data collection parameters were determined based on fluorescence signal from the positive control. Images were oversampled and deconvolved with the Huygens Essential software version 16.10 (Scientific Volume Imaging, The Netherlands, http://svi.nl) after which strong automatic dye separation was applied. All samples and images were treated identically.

2.3.17 Crystal Structure Images. Crystal structure images were color-coded using Chimera.

2.3.18 Statistical Analysis. Statistical analysis was conducted with either a one-way ANOVA with Tukey's post-hoc test or with an unpaired, equal variance, two-tailed t-test. Where indicated, SEM was determined after normalization of each replicate.

2.4 Results

With the goal of identifying PTMs on cell survival signaling nodes, we used, as a starting point, several PTM-specific antibody resins to compare *in vivo* PTMs across multiple mouse tissues (brain, liver, and embryo homogenates). The experimental layout is shown in Figure 2-1A and included several phospho-motif, ubiquitin and acetyl-lysine affinity resins. A complete set of database search results from this experiment are publicly available as a Scaffold file (Proteome Software Inc.) at https://discovery.genome.duke.edu/express/resources/3023/3023_PTMScanAll_withTiO2.sf3. In an effort to zoom in on PTMs on cell survival signaling nodes, we applied gene ontology analysis, as well as manual sorting by protein function. Two proteins of interest, 14-3-3ζ and SOD1, are shown in Figure 2-1B. 14-3-3ζ is a phospho-serine/threonine binding protein that

is overexpressed in a variety of cancers and promotes cell survival by directly modulating a network of phospho-proteins. In combining our PTM data sets, we identified PTMs on 14-3-3ζ of

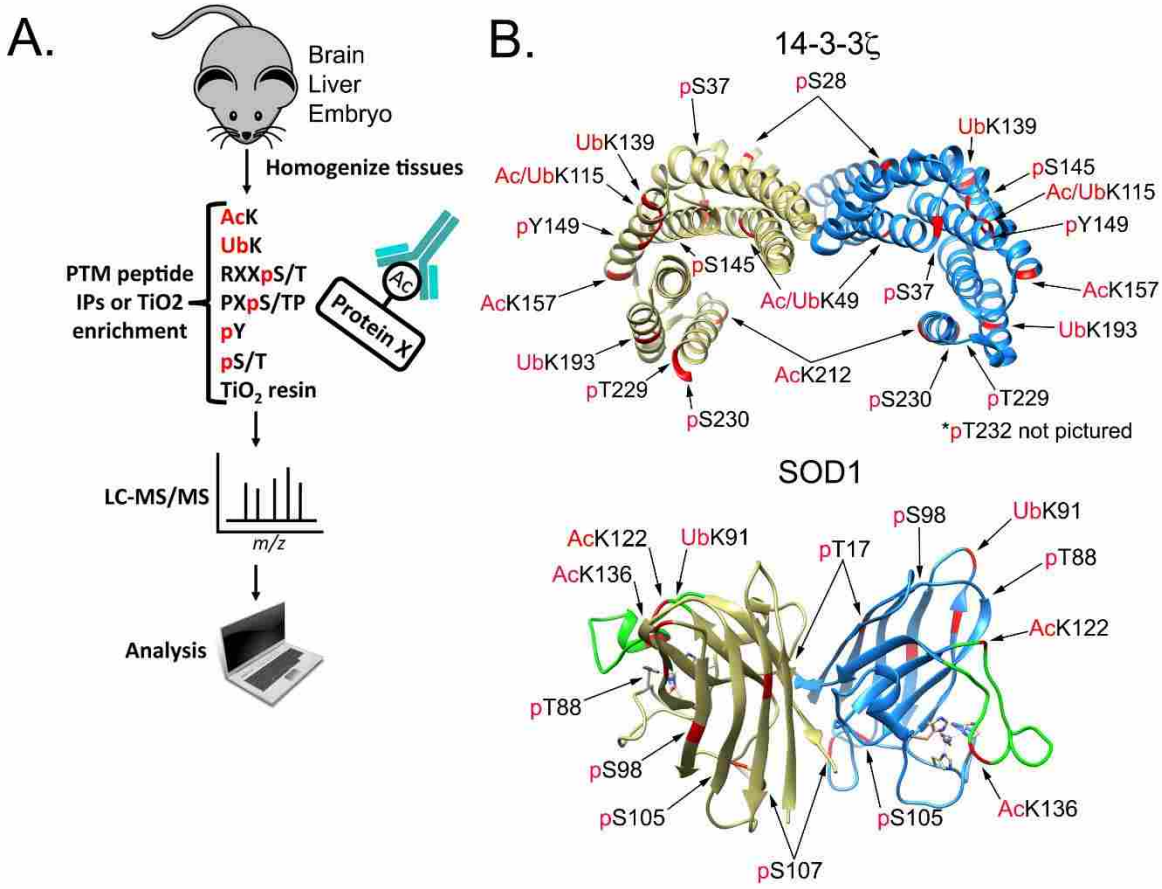

Figure 2-1. Identification of PTMs on 14-3-3ζ and SOD1. (A) Brain, liver, and whole embryo mouse tissues were homogenized and digested with trypsin. Peptides were subject to affinity purification by the indicated antibody resin. Peptides were eluted and analyzed by LC/MS/MS. Proteomics data were analyzed with Scaffold software. **(B)** Crystal structures of human 14-3-3ζ (PDB: 4IHL) and mouse SOD1 (PDB: 3GTT) with PTMs identified in the proteomics data.

unknown function, including phospho-Y149, Ub-K139, in addition to well-described PTMs, such as Ac-K49 [48, 117, 118]. In particular, acetylation of K49 is known to disrupt 14-3-3ζ interactions and our previous work identified HDAC6 as the K49-targeted KDAC [118].

2.4.1 SAPH-ire identifies PTMs with high function potential in the SOD domain family. Our attention was also drawn to SOD1, which acts as one of the main modes of defense against oxidative stress by catalyzing the disproportionation of superoxide radicals (O_2^-) to molecular oxygen (O_2) and hydrogen peroxide (H_2O_2). Figure 2-1B lower panel shows the crystal

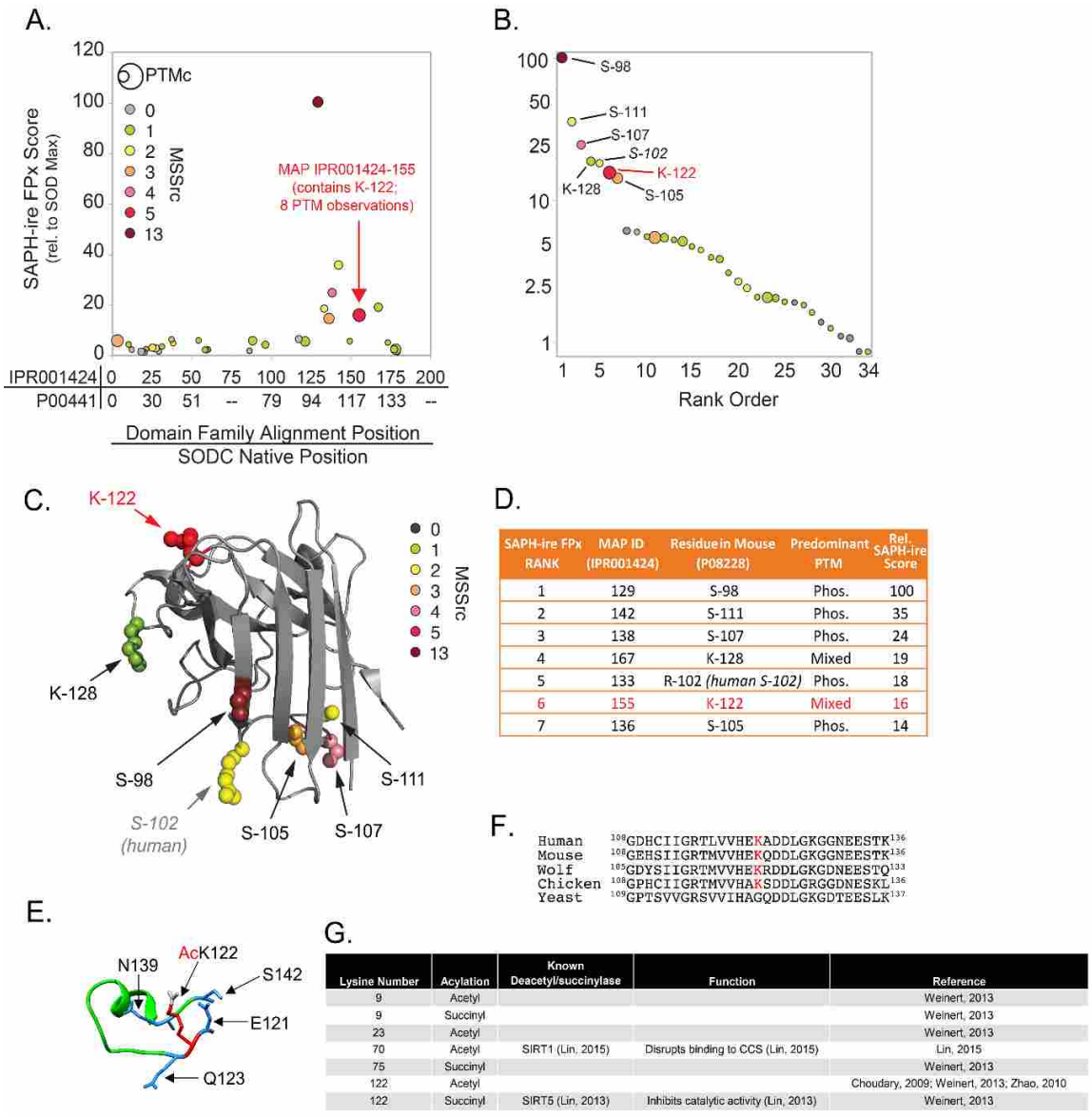

SAPH-ire FPx RANK	MAP ID (IPR001424)	Residue in Mouse (P08228)	Predominant PTM	Rel. SAPH-ire Score
1	129	S-98	Phos.	100
2	142	S-111	Phos.	35
3	138	S-107	Phos.	24
4	167	K-128	Mixed	19
5	133	R-102 *(human S-102)*	Phos.	18
6	155	K-122	Mixed	16
7	136	S-105	Phos.	14

Lysine Number	Acylation	Known Deacetyl/succinylase	Function	Reference
9	Acetyl			Weinert, 2013
9	Succinyl			Weinert, 2013
23	Acetyl			Weinert, 2013
70	Acetyl	SIRT1 (Lin, 2015)	Disrupts binding to CCS (Lin, 2015)	Lin, 2015
75	Succinyl			Weinert, 2013
122	Acetyl			Choudary, 2009; Weinert, 2013; Zhao, 2010
122	Succinyl	SIRT5 (Lin, 2013)	Inhibits catalytic activity (Lin, 2013)	Weinert, 2013

Figure 2-2. SAPH-ire identifies PTMs with high function potential in the SOD domain. (A) Plot of SAPH-ire function potential score for 34 modified alignment positions (MAPs) along the length of the SOD domain family. Domain family alignment position and corresponding native position of human SOD1 are plotted on the x-axis for reference (from N- to C-terminal). The number of distinct PTMs observed within a MAP (PTM count; PTMc) is represented by circle size. The number of independent literature sources documenting observation of PTMs in each MAP (Mass Spec Source Count; MSSrc) is indicated by circle color. **(B)** Rank ordered plot of SAPH-ire function potential scores for the 34 SOD domain family MAPs. Residue positions correspond to mouse SOD1 residues found in each of the top 7 domain family MAPs. **(C)** Projection of the top 7 MAPs onto the crystal structure of mouse SOD1 (UniProt ID: P08228) (PDB: 3GTT, Chain A). **(D)** Table summarizing the identities and predominant PTMs observed for each of the top 7 SOD MAPs. **(E)** Zoomed in crystal structure of the mouse SOD1 (PDB: 3GTT) electrostatic loop featuring K122 (red) modified with an acetyl group (grey) and surrounding amino acids (blue). **(F)** Sequence alignment of human, mouse, wolf, chicken, and yeast SOD1 with K122 highlighted in red. **(G)** Table indicating known lysine acetyl or succinyl modifications of human SOD1, known deacetyl/succinylases, and phenotype of the modifications.

structure of the SOD1 dimer and PTMs identified from our proteomics data. In an effort to prioritize PTMs on SOD1, we utilized SAPH-ire FPx, a machine-learning-based PTM "hotspot" finder that examines experimentally-identified PTMs and prioritizes the PTMs for likelihood of biological function based on a number of parameters as previously described [87-89]. Using human SOD1 (UniProt ID: P00441) as an anchor, PTMs were evaluated in the context of the entire eukaryotic SOD domain family (InterPro ID: IPR001424). Interestingly, PTMs localized in the region between S98 and K128 exhibited the highest SAPH-ire FPx scores across the entire domain (Figure 2-2A). In fact, the top seven PTM sites with the highest FPx score were all within this region (Figure 2-2B-D). We became interested in an acylated lysine (K122) that was found not only in our mouse proteomics data set but was also identified by SAPH-ire in the region with the highest FPx scores and was one of the top two highest ranking modified lysine hotspots in the SOD domain family (Figure 2-2A-D). In comparing the two acyl-lysines (K122 and K128) within the top SAPH-ire cluster, K122 had the highest number (eight) of co-aligned PTMs in the family (indicated by circle size) and also the second highest number (five) of independent MS-based observations (indicated by circle color, Figure 2-2A-C), suggesting that K122 may be an important regulatory site. K122 sits within the electrostatic loop (Figure 2-2E), which has nearby residues (H120 and D124) important for binding zinc and copper [119]. K122 is conserved from human to bird (Figure 2-2F), and has been identified in previous studies, among other acyl-lysines, as acetylated and succinylated [40, 41, 47, 48, 120] (Figure 2-2G). A study by Lin et al. found that SIRT5 desuccinylates K122, and it was proposed to affect SOD1 antioxidant activity [120]. In addition, a recent study using a site-specific antibody demonstrated that K122 is acetylated on endogenous SOD1 in multiple cell types throughout the murine nervous system [44], although the

impact of the acetyl modification on SOD1 function was not demonstrated. With this background, we investigated the functional impact of K122 acylation on SOD1.

2.4.2 Acyl-mimicking mutations at K122 have no effect on SOD1 dimerization or ROS scavenging activity. To examine the effect of acylation at K122 on various SOD1 functions, we generated acetyl-mimicking K122Q and succinyl-mimicking K122E mutations. Although there are structural differences between glutamine/glutamate and N^{ε}-acyl-lysine, these mutations mimic the change in charge associated with the acyl modifications. One limitation of this approach is that the mutations abrogate any other lysine modification (e.g., ubiquitin) that may occur at the site, thus comparison with the K-to-R control (mimics a non-acylated lysine, but also abrogates other lysine PTMs) is critical. To determine whether the acyl-mimicking mutants could dimerize with WT SOD1, we overexpressed Flag-tagged WT SOD1 together with either HA-tagged WT SOD1 or HA-tagged mutant SOD1 in HEK-293 cells and saw no difference in dimerization between WT and acyl-mimicking SOD1 mutants (Figure 2-3A). We also saw no difference in the binding of these SOD1 mutants to the copper chaperone for superoxide dismutase (CCS; Figure 2-3B), which promotes the final stage of SOD1 folding and maturation. Furthermore, in contrast to the study by Lin et al. [120], we found no difference in ROS scavenging between WT and the acyl-mimicking SOD1 mutants. This was verified in multiple ROS scavenging assays with purified SOD1, a nitrotetrazolium blue gel assay, and included the ROS scavenging-impaired SOD1 point mutant G85R, as a positive control (Figures 2-3C and 2-3D).

2.4.3 K122 acyl-mimics inhibit SOD1-mediated control of mitochondrial respiration. Although SOD1 is commonly thought of as an antioxidant, only 1% of SOD1 expressed in cells is necessary to keep ROS below cytotoxic levels [105]. The rationale for such high levels of SOD1 has led others to propose that it may have important functions beyond disproportionation of oxygen

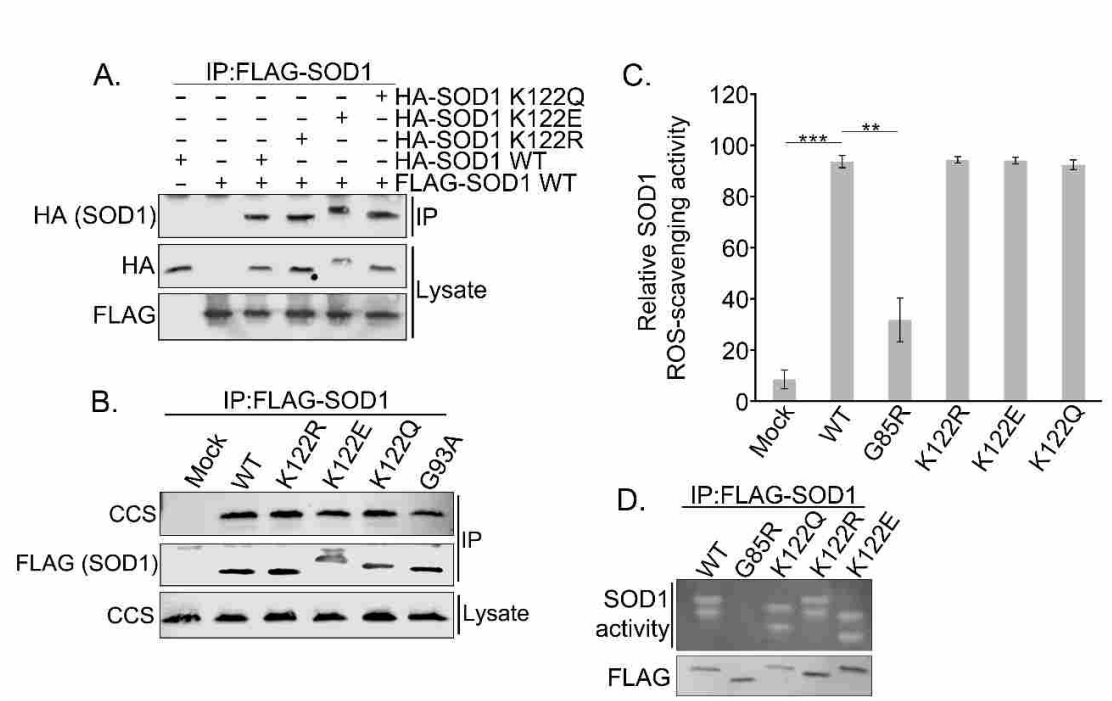

Figure 2-3. Acyl-mimic mutations at K122 of SOD1 do not affect canonical SOD1 ROS scavenging activity. **(A)** HEK 293 cells were co-transfected with Flag-tagged WT SOD1and HA-tagged WT, K122R, K122E, or K122Q SOD1 expression plasmids. Flag-WT SOD1 was immunoprecipitated with Flag agarose resin and run through SDS-PAGE before being immunoblotted for HA-tagged binding partners. **(B)** HEK 293 cells were transfected with Flag-tagged WT, K122R, K122E, K122Q, or G93A SOD1 expression plasmids. Flag-tagged SOD1 was immunoprecipitated with Flag agarose resin and run through SDS-PAGE before being immunoblotted for the CCS binding partner. **(C)** HEK 293 cells were transfected with Flag-tagged WT, G85R, K122R, K122E, or K122Q SOD1. SOD1 was immunoprecipitated with Flag agarose resin and then competitively eluted with Flag peptide. The eluted SOD1 activity was then measured calorimetrically. (n=3; **p<0.01, ***p<0.001; error bars are represented by +/- SEM) **(D)** Samples were prepared as in (C) and the eluted SOD1 was resolved through Native-PAGE and SOD1 activity was assayed within the gel. White bands indicate active SOD1.

radicals [16]. Previous studies have suggested SOD1 has roles in cellular zinc [18] and copper buffering [17], and as a nuclear transcription factor [14, 15]. In addition, a more recent study by Reddi et al. demonstrated a novel function of yeast SOD1 in suppressing mitochondrial respiration through modulation of casein kinase signaling [16]. Given that lysine acylation is linked to metabolism [48, 121, 122], we decided to test the potential link between the K122 PTM and SOD1 anti-respiratory activity. To test whether mammalian SOD1 suppresses respiration like its yeast counterpart, we expressed WT human SOD1 in HEK-293 cells and saw a marked decrease in mitochondrial oxygen flux, suggesting conservation of this SOD1 metabolic function from yeast

to humans (Figure 2-4A). Importantly, in comparing this effect on respiration across the panel of acyl-mimicking SOD1 mutants, we found that the acetyl (K122Q)- and succinyl (K122E)-mimicking mutants completely lost their ability to suppress respiration. Like yeast SOD1, the inhibitory effect of mammalian SOD1 on respiration required its enzymatic activity, as the G85R mutant, which shows ~70% reduced ROS scavenging activity compared to WT (Figure 2-3C), failed to inhibit respiration like WT SOD1 [16]. As an additional control, the K122R mutant was fully active in suppressing respiration, suggesting that the K122Q and K122E phenotypes were not simply due to mutation of the lysine, which could block other lysine PTMs, such as sumoylation or ubiquitination (Figure 2-4A).

To determine which electron transport chain (ETC) subunit complex was affected by SOD1, we treated the SOD1-expressing cells with inhibitors of complex I and II. While complex II does not transport protons across the intermembrane space like complex I, the two complexes work in parallel to transfer electrons to a pool of ubiquinone. Electrons from ubiquinone are then transferred step-wise to complex IV where molecular oxygen is reduced to water. Because complex I and complex II work in parallel to transfer electrons, each can be inhibited separately and electrons can still be transferred through the uninhibited complex. When we inhibited complex II with malonate, SOD1 was still able to suppress respiration. However, when complex I was inhibited with rotenone, SOD1 had no additional effect on respiration (Figure 2-4B), suggesting that SOD1 is inhibiting the ETC at complex I.

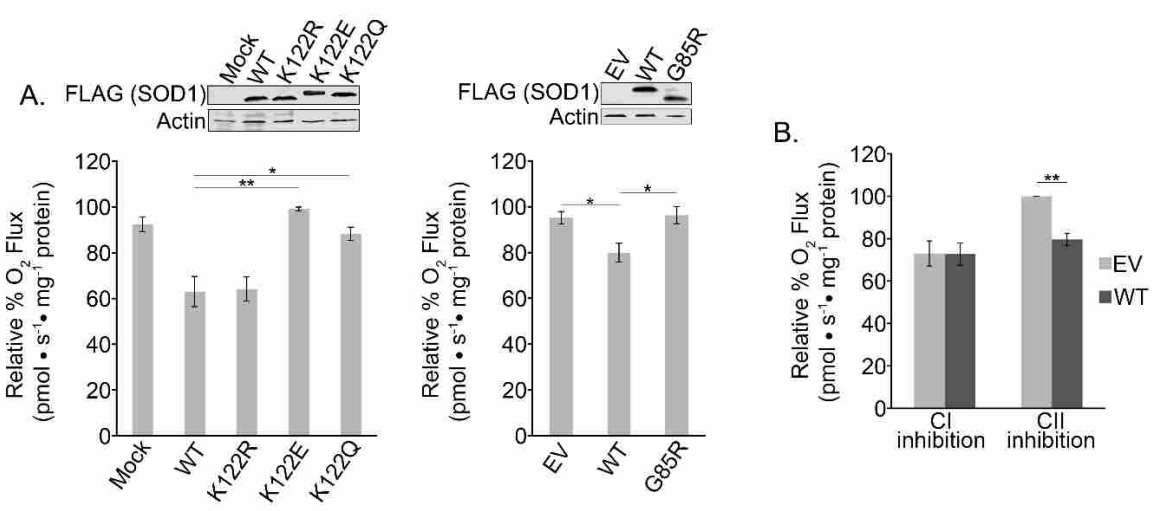

Figure 2-4. Acyl-K122 mimics of SOD1 inhibit SOD1-mediated suppression of mitochondrial respiration. **(A)** Left: HEK 293 cells were transfected with Flag-tagged WT, K122R, K122E, or K122Q SOD1 expression plasmids and oxygen flux was measured with an Oroboros O2K respirometer. Cell lysates were separated by SDS-PAGE and immunoblotted for Flag-SOD1. (n=4; *p<0.05, **p<0.01; error bars are represented by +/- SEM) Right: HEK 293 cells were transfected with an empty vector or Flag-tagged WT, or G85R SOD1 expression plasmids and assayed as in the left panel. (n=3; *p<0.05; error bars are represented by +/- SEM) **(B)** HEK 293 cells were transfected with an empty vector or Flag-tagged WT SOD1 expression vector. Oxygen rates were measured with an Oroboros O2K respirometer after CI inhibition with rotenone (2 mM) or CII inhibition with malonate (2.5 mM). (n=3 technical replicates; **p<0.01; error bars are represented by +/- SEM)

2.4.4 SOD1-mediated inhibition of respiration can be modulated via SIRT5. Lysine acylation is regulated by the activity of lysine deacylases (KDACs), which include the histone deacetylase (HDACs) and Sirtuin families. Unlike many KDACs which prefer acetyl-lysine as their substrate, SIRT5 shows preference toward the longer chain length acylations of succinylation and malonylation [123]. It was previously shown that SIRT5 is the desuccinylase for K122 [120] and, while SIRT5 is traditionally thought of as a mitochondrial Sirtuin, recent studies have described SIRT5's presence in the cytosol as well [124-126]. We validated the role of SIRT5 in desuccinylating K122 by developing an antibody specific for succinylated K122 (Su-K122, Figure 2-5A). To confirm that succinylation occurs on endogenous SOD1, we depleted cells of SIRT5 and immunoprecipitated SOD1. Figure 2-5B shows the increase in endogenous SOD1 succinylation at K122 in SIRT5-depleted cells. Although acetylation of K122 clearly occurs on endogenous SOD1 ([40, 44, 47, 48], proteomics data), our attempts to generate site-specific acetyl-

K122 antibodies resulted in limited success—antibodies showed marginal specificity to the acetylation. This complication, combined with the fact that K122E showed a slightly more robust effect in inhibiting SOD1's anti-respiration function, led us to focus primarily on K122 succinylation.

To determine whether we could block SOD1's anti-respiratory activity by modulating the endogenous deacylation machinery, we depleted SIRT5 in cells expressing WT or the non-succinylatable K122R SOD1 and measured respiration. Remarkably, we found that SIRT5

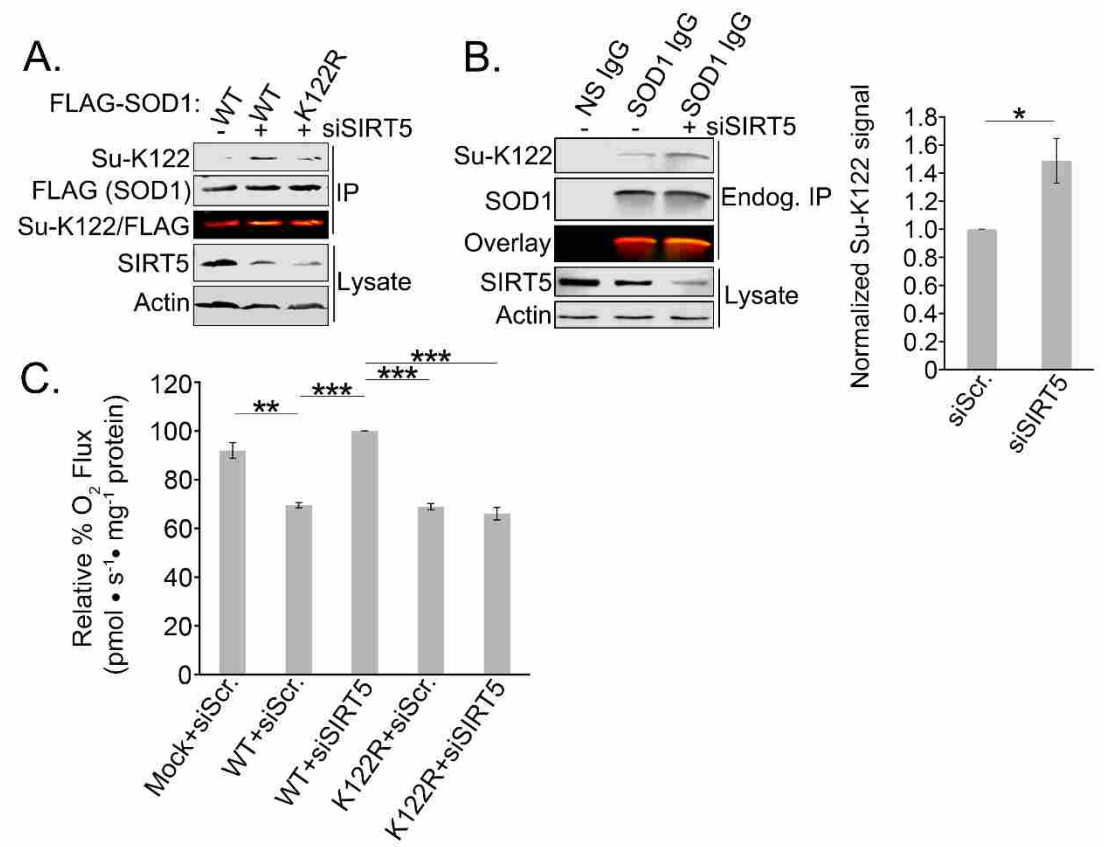

Figure 2-5. Development of an antibody specific to acylated K122 of SOD1; SIRT5 inhibition results in succinylation of endogenous SOD1. (A) Flag-tagged WT or K122R SOD1 was overexpressed in HEK 293 cells with or without SIRT5 knocked down by siRNA. Flag SOD1 was immunoprecipitated with Flag agarose resin, run through SDS-PAGE and immunoblotted for succinyl-K122 (Su-K122) and total (Flag) SOD1. **(B)** Endogenous SOD1 was immunoprecipitated from HEK 293 cells with or without SIRT5 knocked down via siRNA. The immunoprecipitated SOD1 was then run through SDS-PAGE and immunoblotted with Su-K122 antibody. (n=3; *p<0.05; error bars are represented by +/- SEM) **(C)** Flag-tagged WT or K122R SOD1 was overexpressed in HEK 293 cells with or without SIRT5 knocked down by siRNA. Oxygen rates were measured with an Oroboros O2K respirometer. (n=3; **p<0.01, ***p<0.001; error bars are represented by +/- SEM)

depletion recovered normal respiration levels in cells expressing WT SOD1 and the recovery was overridden by the K122R mutant which cannot be acylated (Figure 2-5C). This suggests that SIRT5 modulates metabolism via desuccinylation of SOD1 at K122.

2.4.5 SOD1-mediated suppression of respiration is upstream of its mitochondrial localization. SOD1 is known to reside in the cytosol, IMS of the mitochondria, and the nucleus [127]. Our respiration data made us question whether the anti-respiratory effect of SOD1 is exerted locally within the IMS. If so, we would predict that acylation of K122 blocks SOD1 mitochondrial localization. As shown in Figure 2-6A, we found decreased levels of the acyl-mimicking SOD1 mutants in the mitochondrial fraction. We included the ALS-linked G93A SOD1 mutant as a positive control because it is known to accumulate in the IMS (Figure 2-6A, lane 2) [128]. Shaw and colleagues recently showed that neutralization of positively charged lysines by aspirin-induced lysine acetylation on SOD1 inhibited its propensity to aggregate [50]. However, the acyl-mimicking mutant, in the context of the ALS-linked G93A mutation, did not decrease SOD1 aggregation (Figure 2-6B). Together, these data suggest that acylation at K122 inhibits mitochondrial accumulation of SOD1 and, while only correlative, they raise the possibility that the mitochondrial pool of SOD1 may directly inhibit respiration in the IMS.

Based on these data, our initial hypothesis was that acylation of K122 prevented SOD1 mitochondrial localization and thus blocked SOD1-mediated suppression of respiration. To test this further, we used an approach in which SOD1 is appended, in frame, to the mitochondrial import signal of *Saccharomyces cerevisiae* cytochrome b2 (CytB2) [129]. Our prediction was two-fold: First, that pushing WT SOD1 into the IMS would enhance SOD1-mediated suppression of respiration; and second, that forcing the K122E SOD1 mutant into the mitochondria would rescue its ability to suppress respiration. Figure 2-6C shows validation that the IMS targeting tag resulted

in robust accumulation of WT and K122E SOD1 in the mitochondrial fractions. However, to our surprise, the mitochondrial localization of SOD1 did not enhance its ability to suppress respiration (Figure 2-6D), nor did it recover the ability of the K122E mutant to suppress respiration. This suggests that SOD1's suppression of respiration is independent of its mitochondrial localization, which agrees with data from yeast in which the respiration-suppressing signal from SOD1 originates in the cytosol [16].

An alternative explanation for the relationship between K122 acylation and SOD1 mitochondrial localization is that SOD1's effect on respiration is upstream of its mitochondrial localization. Indeed, there is evidence that the disulfide relay system that imports SOD1 into the IMS is dependent on electron flux through cytochrome c reductase (complex III) of the ETC [130] [131]. Based on this model, up- or down-regulation of respiratory activity would cause a corresponding decrease or increase in SOD1 mitochondrial localization. To test this, we first identified a dose of rotenone, a complex I inhibitor, at 1 nM that produced a 10-15% reduction in overall oxygen consumption (Figure 2-6E), similar to what we had observed with WT SOD1 in our previous experiments. In support of the idea that inhibition of respiration drives mitochondrial uptake of SOD1, treatment of cells with 1 nM rotenone for 30 minutes significantly increased the accumulation of endogenous SOD1 in the mitochondrial pellet (Figure 2-6F). Additionally, treatment of cells with 3-nitropropionic acid (3-NP), a complex II inhibitor, also triggered an increase in mitochondrial SOD1 (Figure 2-6G). Conversely, boosting ETC activity by culturing cells in galactose nearly eliminated the IMS-localized G93A mutant SOD1 from the IMS (Figure 2-6H). These results suggest that cellular respiration levels modulate SOD1 mitochondrial uptake, such that inhibition or stimulation of respiration can toggle SOD1 mitochondrial accumulation up or down, respectively (model in Figure 2-6I). Furthermore, this suggests a potential feedback loop

between SOD1 acylation, inhibition of respiration and SOD1 mitochondrial import (see discussion).

2.4.6 The SOD1 K122E acyl mimic is impaired in its ability to rescue the lethality of SOD1 deletion and reduce mitochondrial ROS levels. While SOD1's vital role in direct disproportionation of cytosolic ROS is well established, our observation that SOD1 suppresses respiration at complex I and the link between respiration and SOD1 mitochondrial import may indicate an added dimension to SOD1's role as an antioxidant. This is based on the decades-old observation that the ETC is a source of ROS [132, 133] and the possible role of the mitochondrial pool of SOD1 in scavenging ROS directly within the IMS [134, 135]. The K122E mutant provided, to our knowledge, the first tool to address this question genetically because it inhibits SOD1's anti-respiratory function while maintaining SOD1 enzymatic ROS scavenging activity. We took advantage of an HCT-116 cell T-REx-based 'flip-in' system wherein a gene of interest can be stably recombined with a specific locus under the control of a doxycycline (dox)-inducible promoter. This provides the advantage of controlling for copy number, which allows for a more fair comparison between different derived lines. After generating a panel of stable doxycycline-inducible SOD1 variants with silent mutations at PAM sites, we used CRISPR/Cas9 to delete endogenous genomic SOD1 from each of the lines. Figure 2-7A shows that the inducible system gives near-endogenous levels of WT and K122E SOD1 expression and is completely refractory to the endogenous SOD1-targeted sgRNA. Of note, we had difficulty immunoblotting for G85R after deletion of SOD1 due to the inability of G85R to rescue cells from the acute toxicity of SOD1 KO.

Previous studies have shown that SOD1 deletion in eukaryotes results in cell death as a result of ROS accumulation [4, 5]. Consistent with this observation, the SOD1 KO lines showed a dramatic loss of cell growth as measured by an Incucyte live cell analysis system (Figure 2-7B–

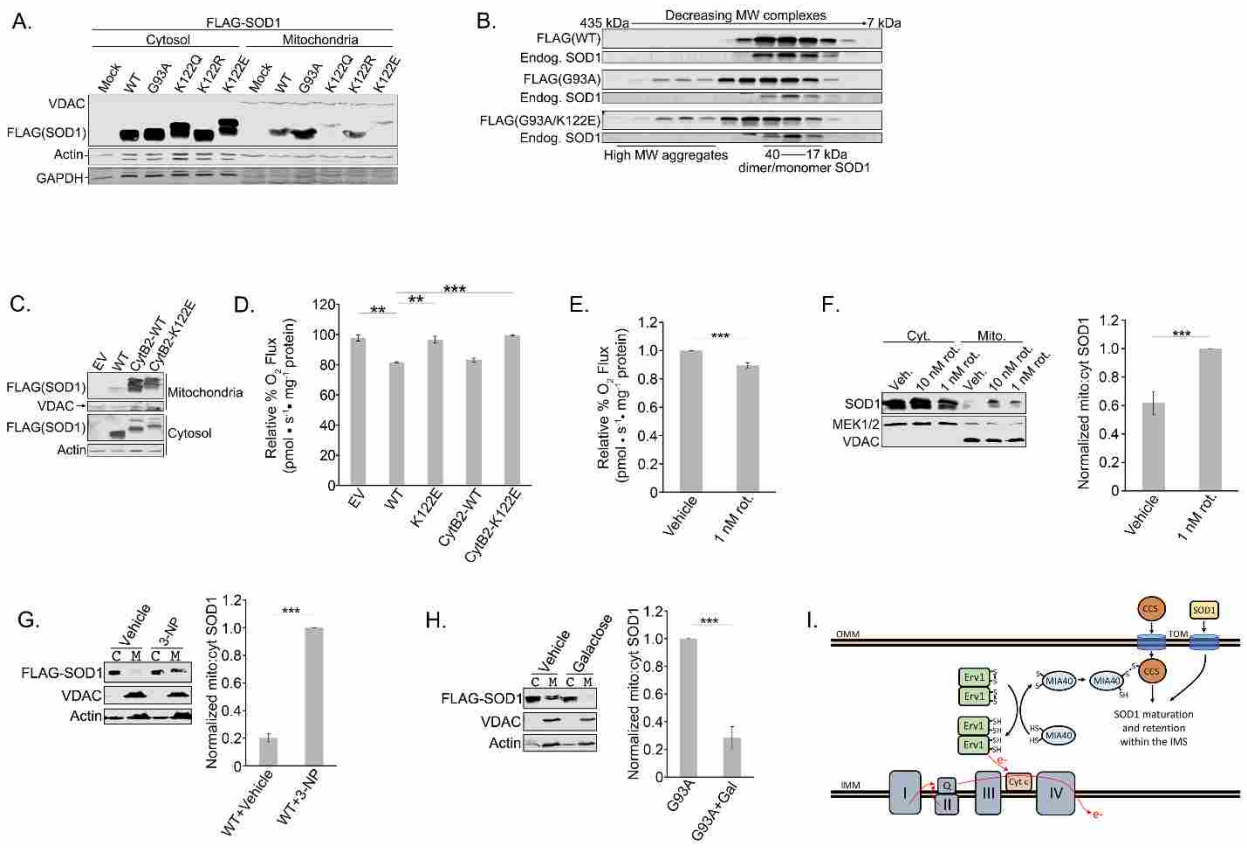

Figure 2-6. SOD1-mediated suppression of respiration is upstream of its mitochondrial localization. (A) HEK 293 cells were transfected with Flag-tagged WT, G93A, K122Q, K122R, or K122E SOD1. The cells were lysed and mitochondria were fractionated from the cytosol. The two fractions were run through SDS-PAGE and immunoblotted for Flag-SOD1 present in the mitochondria vs. the cytosol. **(B)** Flag-tagged WT, G93A, or G93A/K122E SOD1 was induced with tetracycline for 48 hours in T-REx 293 cells. The cells were lysed and the lysates were then loaded onto a Superdex 200 10/300 GL Size exclusion column and eluted in fractions. The fractions were run through SDS-PAGE and immunoblotted for Flag-SOD1 and endogenous SOD1. **(C)** Flag-tagged WT, cytB2-WT, or cytB2-K122E SOD1 was overexpressed in HEK 293 cells. The cells were lysed and mitochondria were fractionated from the cytosol. The two fractions were run through SDS-PAGE and immunoblotted for Flag-SOD1 present in the mitochondria vs. the cytosol. **(D)** Flag-tagged WT, K122E, cytB2-WT, or cytB2-K122E SOD1 was overexpressed in HEK 293 cells. Oxygen rates were measured with an Oroboros O2K respirometer. (n=3; **p<0.01, ***p<0.001; error bars are represented by +/- SEM) **(E)** 1 nM rotenone or vehicle were added to HEK 293 cells 30 minutes prior to measuring oxygen consumption rates with an Oroboros O2K respirometer. (n=4; ***p<0.001; error bars are represented by +/- SEM) **(F)** 1 or 10 nM rotenone or vehicle were added to HEK 293 cells 30 minutes prior to lysing the cells and fractionating the mitochondria from the cytosol as in (A). The fractions were immunoblotted for the presence of endogenous SOD1 in the mitochondria and cytosol. In each replicate, SOD1 levels were normalized to mitochondrial and cytosolic loading controls and then normalized to the ratio of mitochondrial SOD1 in the 1 nM rotenone treated sample. (n=6, ***p<0.001; error bars are represented by +/- SEM) **(G)** Flag-tagged WT-SOD1 was overexpressed in HEK 293 cells. 1 mM 3-nitropropionic acid (3-NP) was added for 16-18 hours before the cells were lysed and mitochondria were fractionated from the cytosol. The two fractions were run through SDS-PAGE and immunoblotted for Flag-SOD1 present in the mitochondria vs. the cytosol. In each replicate, Flag-SOD1 levels were normalized to mitochondrial

and cytosolic loading controls and then normalized to the ratio of mitochondrial Flag-SOD1 in the 3-NP treated sample. (n=3; ***p<0.001; error bars are represented by +/- SEM) **(H)** Flag-tagged G93A-SOD1 was overexpressed in HEK 293 cells. 25 mM galactose in low glucose (2 mM) media was added 24 hours before the cells were lysed and assayed as in (G). In each replicate, Flag-SOD1 levels were normalized to mitochondrial and cytosolic loading controls and then normalized to the ratio of mitochondrial Flag-SOD1 in the untreated sample. (n=3; ***p<0.001; error bars are represented by +/- SEM) **(I)** An Erv1/MIA40 disulfide relay promotes the IMS import of CCS, which in turn promotes the IMS retention of SOD1. The disulfide relay is reset when oxidized cytochrome c accepts an electron from Erv1 (model adapted from Kawamata and Manfredi [2]).

upper panel shows basal growth rates without dox treatment) and infrared scanning of Giemsa-stained cultures after cell dilution and growth over a time course (Figure 2-7C). The loss of growth caused by SOD1 KO was completely reversed in these cells by reconstituting WT SOD1 expression from the dox-inducible locus, indicating that growth defects were not due to off-target effects of the sgRNA. As a control, the G85R mutant, which shows reduced ROS scavenging and does not inhibit respiration, was unable to rescue the growth defect in the SOD1 KO cells. In contrast, SOD1 K122E, which is ROS scavenging-active but defective in inhibition of respiration, showed an intermediate rescue of growth. JC-1 staining for mitochondrial membrane potential showed a similar trend with a dramatic loss of membrane potential, a hallmark of oxidative stress, in the SOD1 KO and G85R addback lines and a partial rescue of mitochondrial function in the K122E-expressing cells (Figure 2-7D). To measure ROS levels directly within the mitochondria of each treatment, we used the MitoSOX mitochondrial ROS probe. Flow cytometric quantitation of mitochondrial ROS mirrored the proliferation and JC-1 results, with WT SOD1 rescuing the increase of mitochondrial ROS caused by SOD1 KO, and the K122E mutant showing a partial rescue (Figure 2-7E). Representative confocal images of this experiment are shown in Figure 2-7F. Together, these data suggest that SOD1-mediated dampening of respiration contributes to SOD1-mediated cell survival. Possible mechanisms to explain this effect are discussed below.

2.5 Discussion

We began this study with several affinity purification-based proteomics approaches to identify PTMs across multiple tissues with the primary goal of finding new mechanisms of regulation on cell survival signaling nodes. All proteomics data from this effort is freely available (see link below under proteomics description). By using the machine learning approach of SAPH-ire [89], we prioritized several SOD1 PTMs for future study. Notably, a phosphorylation at S98 (or S99 depending on numbering scheme) showed the highest SAPH-ire score. This phosphorylation sits within a solvent-exposed beta sheet of SOD1 and has been shown to regulate SOD1's role in transcription [14]. It is also notable that seven SOD1 PTMs were grouped within a high SAPH-ire score cluster, and all sit within a relatively small region spanning S98 to K128, which includes part of the electrostatic loop.

We focused our initial studies on an acetylation within the electrostatic loop of SOD1 at K122. This lysine was intriguing for several reasons. First, of the acylated lysines within the top SAPH-ire cluster, it had the highest number of independent MS identifications (Figure 2-2A). Second, it was conserved across multicellular eukaryotes and positioned within a known functional region of SOD1. Third, we had previously identified this lysine as a Sirtuin substrate using a biotin-switch approach in *Xenopus* egg extract [117], so its appearance in our proteomics data from mouse tissue was striking. Lastly, during the course of this project, Lin and colleagues confirmed the site as succinylated, which corroborated the lysine as a potentially important site of regulation, as lysines that are acetylated are also commonly succinylated [40].

Two observations shed light on the potential mechanism by which acylation at K122 inhibits SOD1-mediated suppression of respiration. First, we found that the ROS scavenging-impaired SOD1 G85R mutant fails to suppress respiration, which agrees with data from yeast that ROS scavenging enzymatic activity is required for this new SOD1 function [16]. Second, we

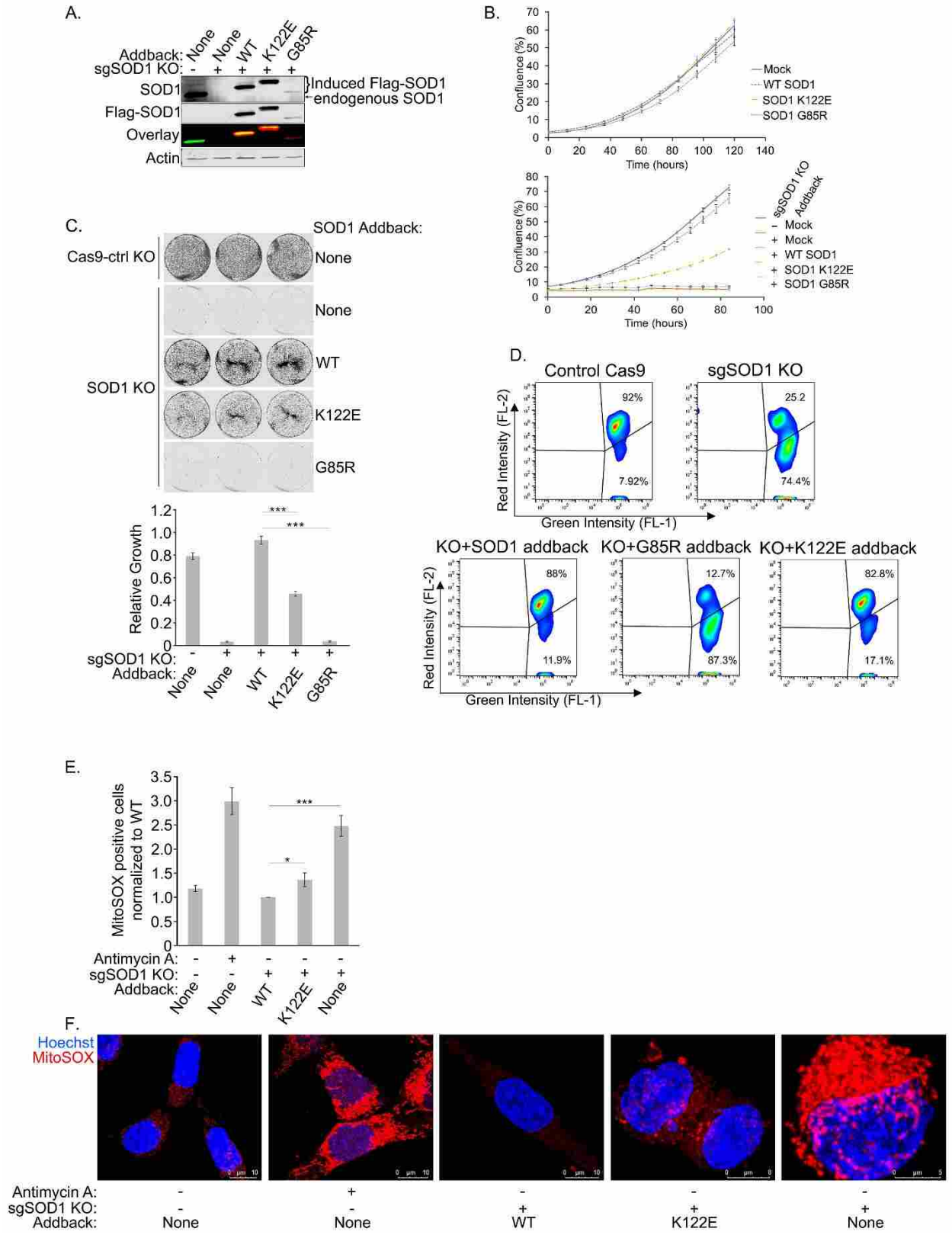
A.
Addback: None None WT K122E G85R
sgSOD1 KO: - + + + +
SOD1
Flag-SOD1
Overlay
Actin
Induced Flag-SOD1
endogenous SOD1
B.
Confluence (%)
Time (hours)
Mock
WT SOD1
SOD1 K122E
SOD1 G85R
sgSOD1 KO Addback
C.
SOD1 Addback:
Cas9-ctrl KO
None
SOD1 KO
None
WT
K122E
G85R
Relative Growth
sgSOD1 KO:
Addback:
D.
Control Cas9
sgSOD1 KO
92%
7.92%
25.2
74.4%
Red Intensity (FL-2)
Green Intensity (FL-1)
KO+SOD1 addback
KO+G85R addback
KO+K122E addback
88%
11.9%
12.7%
87.3%
82.8%
17.1%
E.
MitoSOX positive cells normalized to WT
Antimycin A:
sgSOD1 KO:
Addback:
F.
Hoechst
MitoSOX
Antimycin A:
sgSOD1 KO:
Addback:
None
None
WT
K122E
None

Figure 2-7. The SOD1 K122E acyl mimic is impaired in its ability to rescue the lethality of SOD1 deletion and reduce mitochondrial ROS levels. (A) Endogenous SOD1 was knocked out of HCT-116 T-REx cells using the CRISPR-Cas9 system. Expression of Flag-tagged SOD1 (with a mutated PAM site) was induced in the T-REx cells with Doxycycline. The cells were lysed and subjected to SDS-PAGE before being immunoblotted for endogenous SOD1 and overexpressed Flag-tagged SOD1. **(B)** Upper: SOD1 HCT-116 T-REx cells were seeded in 24-well plates and grown in the absence of doxycycline. Cell confluence was measured by an Incucyte Zoom. (n=4 technical replicates; error bars are represented by +/- SEM) Lower: SOD1 was knocked out as in (A) and plated and analyzed as in (B; upper). **(C)** After knockout of endogenous SOD1 and overexpression of Flag-tagged SOD1, the HCT-116 T-REx cells were seeded at 22,500 cells per well and allowed to grow for 4 days before being fixed and stained with Giemsa. The wells were then imaged and quantified. (n=3 technical replicates; ***$p<0.001$; error bars are represented by +/- SEM) **(D)** Cells prepared as in (B) lower panel were stained with JC-1 to measure mitochondrial membrane potential. A live-cell population was gated from FSC and SSC measurements, and FL-1 was plotted against FL-2. Higher FL-2:FL-1 ratio indicates higher (healthier) mitochondrial membrane potential. **(E)** Cells prepared as in (B) lower panel were stained with MitoSOX Red to measure mitochondrial superoxide content. A live-cell population was gated from FSC and SSC measurements, from which a population of singlets was identified and selected. A threshold for positive MitoSOX stain was set based on the unstained control and a ratio of BL-3-positive cells to singlets was calculated and normalized to WT-add back cells. Higher ratio indicates larger proportion of cells with superoxide present. (n=4; *$p<0.05$, ***$p<0.001$; error bars are represented by +/- SEM) **(F)** Cells prepared as in (B) lower panel were stained with 5 μM MitoSOX Red for 10 minutes, and nuclei were counterstained. Prior to MitoSOX staining, positive control cells were treated with 30 μM antimycin A for 40 minutes.

found that the acyl-mutants of SOD1, K122E and K122Q, fail to suppress respiration yet have fully functional ROS scavenging enzymatic activity, which we confirmed through multiple assays. In aligning these two observations, we reasoned that acylation at K122 may disrupt a protein-protein interaction critical for suppressing respiration. Based on data from yeast, a clear candidate SOD1 interactor is CK1γ [16]. Unlike its yeast counterpart, human CK1γ has no clear analogous C-terminal degron and we were unable to see the interaction by co-IP in human cells (limited by antibodies with poor specificity). However, there are several isoforms of human casein kinase and, interestingly, a sequence roughly matching the yeast CK1γ degron exists in the alpha isoform. Ongoing efforts are exploring these possibilities. Furthermore, we attempted unbiased co-IP proteomics to identify proteins that differentially interacted with SOD1 WT versus the K122E mutant, but these provided strikingly few proteins (data not shown). In consulting with others in the SOD1 field, this appears to be a fairly common observation and may indicate the need for cross-linking or other approaches to stabilize SOD1-interacting proteins for capture. Nevertheless,

our data support the idea that K122 acylation disrupts a SOD1 interaction that is critical for suppression of respiration and our future efforts will focus on this mechanism.

In searching for a mechanism to explain the ability of K122 acylation to regulate SOD1's anti-respiratory activity, we found that acyl-mimicking SOD1 mutants differed from WT SOD1 in that they failed to accumulate in mitochondria. This result initially led us to think that the acyl-K122 mutants failed to suppress respiration because they were unable to accumulate within the IMS, where we presumed they were directly inhibiting the ETC. However, we found that forcing the K122E mutant into the IMS with an IMS-targeting tag failed to recover its ability to suppress respiration. In addition, the IMS-targeting tag did not confer additional respiration-suppressing activity to WT SOD1. Nevertheless, this initially surprising result actually agrees with data from Reddi and Culotta, in which they showed that yeast SOD1 suppresses mitochondrial respiration from the cytosol by interacting with and stabilizing CK1γ [16].

Our observation that forcing the K122E mutant back into the mitochondria failed to recover its ability to suppress respiration caused us to reconsider how SOD1 acylation and IMS accumulation could be linked. Previous work suggests that the import of SOD1 into the IMS depends on an Erv1/Mia40 disulfide relay system (reviewed in [2]). The activity of this disulfide system is dependent on the oxidation of Erv1 by oxidized cytochrome c [136, 137]. Therefore, under conditions in which respiration is highly active, the ratio of reduced-to-oxidized cytochrome c should increase, leading to a corresponding decrease in Erv1 oxidation and SOD1 mitochondrial import. Conversely, a drop in respiration (causing a build-up of oxidized cytochrome c) would increase SOD1 import into the IMS. In support of this model, we found that inhibiting respiration led to accumulation of SOD1 in mitochondria fractions, while boosting respiration with galactose caused a decrease in mitochondrial SOD1. Similar results have been observed in astrocytes [138].

Taken together with the IMS phenotype of the acyl-SOD1 mutants, we favor the model that acylation of SOD1 is upstream of SOD1 import into the IMS. Acylation of SOD1 blocks its anti-respiratory function, which in turn decreases its import into the IMS. Conversely, we posit that SOD1's ability to suppress respiration feeds forward to drive its own IMS import and acylation may serve as a brake on this mechanism.

In the bigger picture, an intriguing implication of this model is a potentially expanded view of SOD1-mediated anti-oxidant defense–That SOD1-mediated suppression of respiration contributes to its antioxidant/pro-survival function (see model in Figure 2-8). This could occur through at least two possible mechanisms: 1) Inhibition of respiration drives SOD1 into the mitochondria, placing SOD1 directly in position to scavenge ROS as it leaks from complex III. In support of this idea, elevated mitochondrial SOD1 increases cell viability in a yeast system [135] and mitochondria-targeted SOD1 rescues the loss of mitochondrial density observed in SOD1 null mice [134]. This model is intriguing as a variety of stresses, such as ischemia/reperfusion and cell toxins, place strain on mitochondrial respiration and are known to cause spikes in mitochondrial ROS [139]. 2) Alternatively, the dampening of respiration at complex I by SOD1 may inhibit ROS production directly. Interestingly, genetic inhibition of respiration partially rescues the loss of viability caused by SOD1 deletion in yeast [140]. Furthermore, metformin is known to suppress mitochondrial ROS via inhibition of complex I [141-143]. Exactly how this may occur is more puzzling as our understanding of ROS generation from the ETC, and complex I in particular, is limited. Prevailing dogma suggests that complex I only releases ROS into the matrix, but depending on the point at which complex I is inhibited, it could dampen the reduction of semiquinones or Fe-S clusters that may generate O_2^- elsewhere [144] or may simply reduce the

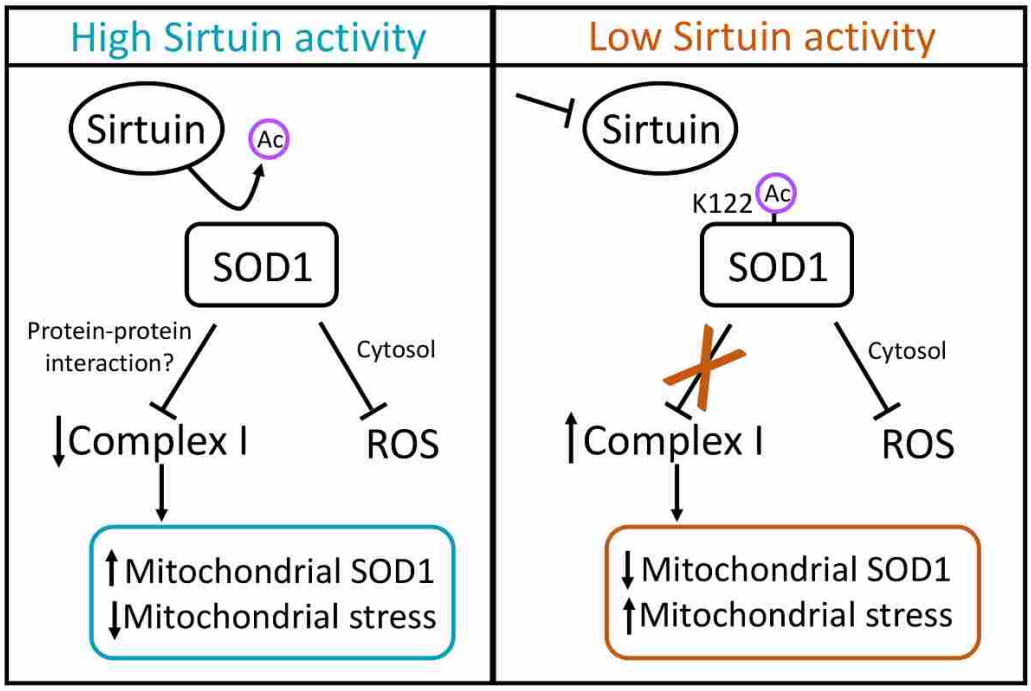

Figure 2-8. Model. High levels of Sirtuin activity (SIRT5 for SOD1 succinylation) deacylate SOD1, which activates SOD1's respiration-suppressing activity at complex I. We posit that SOD1-mediated inhibition of respiration contributes to SOD1-mediated cell survival through two potential (non-mutually exclusive) mechanisms: 1) Inhibition of respiration increases the mitochondrial pool of SOD1, placing SOD1 directly in position to scavenge ROS leaking into the IMS; 2) Dampening of respiration may directly reduce the production of ROS from the ETC.

flow of electrons to complex III, a key producer of ROS within the IMS [139].

We found that the impaired growth of SOD1 null cells, known to be caused by accumulation of oxidative damage [4, 11, 99, 100, 140], could only be partially rescued by the SOD1 K122E mutant, which is catalytically active against ROS but defective in inhibiting respiration. Taken together, our data suggest that SOD1-mediated inhibition of respiration, while clearly not the entire picture, may contribute to SOD1-mediated cell survival. Furthermore, the link between IMS import of SOD1 and respiratory activity suggests a feedback loop in which additional SOD1 may be recruited into mitochondria under conditions (e.g., mitochondrial damage leading to ROS production) in which reinforced ROS scavenging would be needed.

In summary, our data identifies, to our knowledge, the first acylation on SOD1 that regulates its ability to suppress mitochondrial respiration. Given that Sirtuin activity is linked to NAD^+ levels, which, in turn, are linked to the overall metabolic state of the cell, SOD1 acylation may act as a sensor to link nutrient metabolism to SOD1-mediated suppression of respiration. As described above, this may provide an additional dimension to SOD1 antioxidant defense. These data raise additional questions: Does SOD1 acylation disrupt a protein-protein interaction that transmits the signal to complex I? Given that our data suggest that dampened respiration promotes SOD1 mitochondrial import, could the toxic mitochondrial accumulation of ALS-linked SOD1 mutants in neurons be caused by an underlying perturbation of mitochondrial metabolism in a feed forward loop? Answers to these and other related questions will help shed light on the increasingly complex picture of SOD1 biology.

2.6 Acknowledgements

We thank Drs. Giovanni Manfredi and Dennis Winge for their guidance in SOD1 biology. We thank Drs. Jonathan Alder and JC Price for excellent technical help and key reagents. We thank Cell Signaling Technology, Inc., specifically Dr. Jeff Silva and Charles Farnsworth, for providing the PTM antibody resins for proteomics. We thank all members of the Andersen laboratory for constructive discussion and analysis of data. We thank the Fritz B. Burns Foundation (gift to JLA), the National Institutes of Health (R15CA202619 to JLA and R01GM117400 to MPT), and the Simmons Center for Cancer Research (fellowships to CJB and NWR) for funding.

2.7 Author Contributions

CJB and NWR conceived/performed experiments and wrote manuscript. KRG performed experiments. JBM and MTW helped initiate project and provided key laboratory support. RP and

MPT performed SAPH-ire analysis. BTB and JST provided support with metabolic assays. EJS, JWT, and MAM executed proteomics experiments. ARR provided guidance throughout the course of the project. JLA conceived experiments and wrote manuscript.

REFERENCES

1. Banks, C.J., Rodriguez, N.W., Gashler, K.R., Pandya, R., Mortenson, J.B., Whited, M.D., Soderblom, E.J., Thompson, J.W., Moseley, M.A., Reddi, A.R., Tessem, J.S., Torres, M.P., Bikman, B.T. & Andersen, J.L., *Acylation of Superoxide Dismutase 1 (SOD1) at K122 Governs SOD1-mediated Inhibition of Mitochondrial Respiration.* Molecular and Cellular Biology, In Press.
2. Kawamata, H. and G. Manfredi, *Import, maturation, and function of SOD1 and its copper chaperone CCS in the mitochondrial intermembrane space.* Antioxid Redox Signal, 2010. **13**(9): p. 1375-84.
3. McCord, J.M. and I. Fridovich, *Superoxide dismutase. An enzymic function for erythrocuprein (hemocuprein).* J Biol Chem, 1969. **244**(22): p. 6049-55.
4. De Freitas, J.M., et al., *Yeast lacking Cu-Zn superoxide dismutase show altered iron homeostasis. Role of oxidative stress in iron metabolism.* J Biol Chem, 2000. **275**(16): p. 11645-9.
5. Inoue, E., et al., *SOD1 Is Essential for the Viability of DT40 Cells and Nuclear SOD1 Functions as a Guardian of Genomic DNA.* J Nucleic Acids, 2010. **2010**.
6. Corson, L.B., et al., *Chaperone-facilitated copper binding is a property common to several classes of familial amyotrophic lateral sclerosis-linked superoxide dismutase mutants.* Proc Natl Acad Sci U S A, 1998. **95**(11): p. 6361-6.
7. Kruman, II, et al., *ALS-linked Cu/Zn-SOD mutation increases vulnerability of motor neurons to excitotoxicity by a mechanism involving increased oxidative stress and perturbed calcium homeostasis.* Exp Neurol, 1999. **160**(1): p. 28-39.
8. Famulari, A.L., et al., *The antioxidant enzymatic blood profile in Alzheimer's and vascular diseases. Their association and a possible assay to differentiate demented subjects and controls.* J Neurol Sci, 1996. **141**(1-2): p. 69-78.
9. Ihara, Y., et al., *Hydroxyl radical and superoxide dismutase in blood of patients with Parkinson's disease: relationship to clinical data.* J Neurol Sci, 1999. **170**(2): p. 90-5.
10. Somwar, R., et al., *Superoxide dismutase 1 (SOD1) is a target for a small molecule identified in a screen for inhibitors of the growth of lung adenocarcinoma cell lines.* Proceedings of the National Academy of Sciences of the United States of America, 2011. **108**(39): p. 16375-16380.
11. Glasauer, A., et al., *Targeting SOD1 reduces experimental non-small-cell lung cancer.* Journal of Clinical Investigation, 2014. **124**(1): p. 117-128.
12. Papa, L., et al., *SOD2 to SOD1 Switch in Breast Cancer.* Journal of Biological Chemistry, 2014. **289**(9): p. 5412-5416.
13. Papa, L., Manfredi, G. & Germain, D., *SOD1, an unexpected novel target for cancer therapy.* Genes & Cancer, 2014. **5**: p. 15-21.
14. Tsang, C.K., et al., *Superoxide dismutase 1 acts as a nuclear transcription factor to regulate oxidative stress resistance.* Nat Commun, 2014. **5**: p. 3446.
15. Wood, L.K. and D.J. Thiele, *Transcriptional activation in yeast in response to copper deficiency involves copper-zinc superoxide dismutase.* J Biol Chem, 2009. **284**(1): p. 404-13.
16. Reddi, A.R. and V.C. Culotta, *SOD1 integrates signals from oxygen and glucose to repress respiration.* Cell, 2013. **152**(1-2): p. 224-35.

17. Culotta, V.C., et al., *A physiological role for Saccharomyces cerevisiae copper/zinc superoxide dismutase in copper buffering.* J Biol Chem, 1995. **270**(50): p. 29991-7.
18. Wei, J.P., et al., *Evidence for a novel role of copper-zinc superoxide dismutase in zinc metabolism.* J Biol Chem, 2001. **276**(48): p. 44798-803.
19. Takamiya, R., et al., *Overexpression of mutated Cu,Zn-SOD in neuroblastoma cells results in cytoskeletal change.* Am J Physiol Cell Physiol, 2005. **288**(2): p. C253-9.
20. Vigilanza, P., et al., *Transient cytoskeletal alterations after SOD1 depletion in neuroblastoma cells.* Cell Mol Life Sci, 2008. **65**(6): p. 991-1004.
21. Wilcox, K.C., et al., *Modifications of Superoxide Dismutase (SOD1) in Human Erythrocytes A POSSIBLE ROLE IN AMYOTROPHIC LATERAL SCLEROSIS.* Journal of Biological Chemistry, 2009. **284**(20): p. 13940-13947.
22. Khare, S.D. and N.V. Dokholyan, *Common dynamical signatures of familial amyotrophic lateral sclerosis-associated structurally diverse Cu, Zn superoxide dismutase mutants.* Proceedings of the National Academy of Sciences of the United States of America, 2006. **103**(9): p. 3147-3152.
23. Bredesen, D.E., et al., *Do posttranslational modifications of CuZnSOD lead to sporadic amyotrophic lateral sclerosis?* Ann Neurol, 1997. **42**(2): p. 135-7.
24. Kabashi, E., et al., *Oxidized/misfolded superoxide dismutase-1: the cause of all amyotrophic lateral sclerosis?* Ann Neurol, 2007. **62**(6): p. 553-9.
25. Rakhit, R., et al., *Monomeric Cu,Zn-superoxide dismutase is a common misfolding intermediate in the oxidation models of sporadic and familial amyotrophic lateral sclerosis.* J Biol Chem, 2004. **279**(15): p. 15499-504.
26. Rakhit, R., et al., *Oxidation-induced misfolding and aggregation of superoxide dismutase and its implications for amyotrophic lateral sclerosis.* J Biol Chem, 2002. **277**(49): p. 47551-6.
27. Shibata, N., et al., *Cu/Zn superoxide dismutase-like immunoreactivity in Lewy body-like inclusions of sporadic amyotrophic lateral sclerosis.* Neurosci Lett, 1994. **179**(1-2): p. 149-52.
28. Choi, J., et al., *Oxidative modifications and aggregation of Cu,Zn-superoxide dismutase associated with Alzheimer and Parkinson diseases.* Journal of Biological Chemistry, 2005. **280**(12): p. 11648-11655.
29. Hunter, T., *Tyrosine phosphorylation: thirty years and counting.* Curr Opin Cell Biol, 2009. **21**(2): p. 140-6.
30. Ciechanover, A., *Proteolysis: from the lysosome to ubiquitin and the proteasome.* Nat Rev Mol Cell Biol, 2005. **6**(1): p. 79-87.
31. Deribe, Y.L., T. Pawson, and I. Dikic, *Post-translational modifications in signal integration.* Nat Struct Mol Biol, 2010. **17**(6): p. 666-72.
32. Bononi, A., et al., *Protein kinases and phosphatases in the control of cell fate.* Enzyme Res, 2011. **2011**: p. 329098.
33. Hjornevik, L.V., et al., *Nodularin Exposure Induces SOD1 Phosphorylation and Disrupts SOD1 Co-localization with Actin Filaments.* Toxins, 2012. **4**(12): p. 1482-1499.
34. Csar, X.F., et al., *Copper/zinc superoxide dismutase is phosphorylated and modulated specifically by granulocyte-colony stimulating factor in myeloid cells.* Proteomics, 2001. **1**(3): p. 435-443.
35. Fay, J.M., et al., *A Phosphomimetic Mutation Stabilizes SOD1 and Rescues Cell Viability in the Context of an ALS-Associated Mutation.* Structure, 2016. **24**(11): p. 1898-1906.

36. Leitch, J.M., et al., *Post-Translational Modification of Cu/Zn Superoxide Dismutase under Anaerobic Conditions.* Biochemistry, 2012. **51**(2): p. 677-685.
37. Wagner, G.R. and M.D. Hirschey, *Nonenzymatic protein acylation as a carbon stress regulated by sirtuin deacylases.* Mol Cell, 2014. **54**(1): p. 5-16.
38. Wagner, G.R. and R.M. Payne, *Widespread and enzyme-independent Nepsilon-acetylation and Nepsilon-succinylation of proteins in the chemical conditions of the mitochondrial matrix.* J Biol Chem, 2013. **288**(40): p. 29036-45.
39. Weinert, B.T., et al., *Acetylation dynamics and stoichiometry in Saccharomyces cerevisiae.* Mol Syst Biol, 2015. **11**(10): p. 833.
40. Weinert, B.T., et al., *Lysine succinylation is a frequently occurring modification in prokaryotes and eukaryotes and extensively overlaps with acetylation.* Cell Rep, 2013. **4**(4): p. 842-51.
41. Lin, C., et al., *Acetylation at lysine 71 inactivates superoxide dismutase 1 and sensitizes cancer cells to genotoxic agents.* Oncotarget, 2015. **6**(24): p. 20578-91.
42. Getzoff, E.D., et al., *Electrostatic recognition between superoxide and copper, zinc superoxide dismutase.* Nature, 1983. **306**(5940): p. 287-90.
43. Getzoff, E.D., et al., *Faster superoxide dismutase mutants designed by enhancing electrostatic guidance.* Nature, 1992. **358**(6384): p. 347-51.
44. Kaliszewski, M., et al., *SOD1 Lysine 123 Acetylation in the Adult Central Nervous System.* Front Cell Neurosci, 2016. **10**: p. 287.
45. Mertins, P., et al., *Integrated proteomic analysis of post-translational modifications by serial enrichment.* Nat Methods, 2013. **10**(7): p. 634-7.
46. Beli, P., et al., *Proteomic investigations reveal a role for RNA processing factor THRAP3 in the DNA damage response.* Mol Cell, 2012. **46**(2): p. 212-25.
47. Zhao, S., et al., *Regulation of cellular metabolism by protein lysine acetylation.* Science, 2010. **327**(5968): p. 1000-4.
48. Choudhary, C., et al., *Lysine acetylation targets protein complexes and co-regulates major cellular functions.* Science, 2009. **325**(5942): p. 834-40.
49. Lin, Z.F., et al., *SIRT5 desuccinylates and activates SOD1 to eliminate ROS.* Biochem Biophys Res Commun, 2013. **441**(1): p. 191-5.
50. Abdolvahabi, A., et al., *Arresting amyloid with coulomb's law: acetylation of ALS-linked SOD1 by aspirin impedes aggregation.* Biophys J, 2015. **108**(5): p. 1199-212.
51. Swatek, K.N. and D. Komander, *Ubiquitin modifications.* Cell Res, 2016. **26**(4): p. 399-422.
52. Geiss-Friedlander, R. and F. Melchior, *Concepts in sumoylation: a decade on.* Nat Rev Mol Cell Biol, 2007. **8**(12): p. 947-56.
53. Fei, E., et al., *SUMO-1 modification increases human SOD1 stability and aggregation.* Biochem Biophys Res Commun, 2006. **347**(2): p. 406-12.
54. Zhou, W., J.J. Ryan, and H. Zhou, *Global analyses of sumoylated proteins in Saccharomyces cerevisiae. Induction of protein sumoylation by cellular stresses.* J Biol Chem, 2004. **279**(31): p. 32262-8.
55. Kabuta, T., Y. Suzuki, and K. Wada, *Degradation of amyotrophic lateral sclerosis-linked mutant Cu,Zn-superoxide dismutase proteins by macroautophagy and the proteasome.* J Biol Chem, 2006. **281**(41): p. 30524-33.
56. Kato, S., et al., *Pathological characterization of astrocytic hyaline inclusions in familial amyotrophic lateral sclerosis.* Am J Pathol, 1997. **151**(2): p. 611-20.

57. Bruijn, L.I., et al., *ALS-linked SOD1 mutant G85R mediates damage to astrocytes and promotes rapidly progressive disease with SOD1-containing inclusions.* Neuron, 1997. **18**(2): p. 327-38.
58. Stieber, A., J.O. Gonatas, and N.K. Gonatas, *Aggregation of ubiquitin and a mutant ALS-linked SOD1 protein correlate with disease progression and fragmentation of the Golgi apparatus.* J Neurol Sci, 2000. **173**(1): p. 53-62.
59. Basso, M., et al., *Insoluble mutant SOD1 is partly oligoubiquitinated in amyotrophic lateral sclerosis mice.* J Biol Chem, 2006. **281**(44): p. 33325-35.
60. Ganesan, S., et al., *Mutant SOD1 detoxification mechanisms in intact single cells.* Cell Death Differ, 2008. **15**(2): p. 312-21.
61. Bruening, W., et al., *Up-regulation of protein chaperones preserves viability of cells expressing toxic Cu/Zn-superoxide dismutase mutants associated with amyotrophic lateral sclerosis.* J Neurochem, 1999. **72**(2): p. 693-9.
62. Tummala, H., et al., *Inhibition of chaperone activity is a shared property of several Cu,Zn-superoxide dismutase mutants that cause amyotrophic lateral sclerosis.* J Biol Chem, 2005. **280**(18): p. 17725-31.
63. Niwa, J., et al., *Dorfin ubiquitylates mutant SOD1 and prevents mutant SOD1-mediated neurotoxicity.* J Biol Chem, 2002. **277**(39): p. 36793-8.
64. Miyazaki, K., et al., *NEDL1, a novel ubiquitin-protein isopeptide ligase for dishevelled-1, targets mutant superoxide dismutase-1.* J Biol Chem, 2004. **279**(12): p. 11327-35.
65. Yonashiro, R., et al., *Mitochondrial ubiquitin ligase MITOL ubiquitinates mutant SOD1 and attenuates mutant SOD1-induced reactive oxygen species generation.* Mol Biol Cell, 2009. **20**(21): p. 4524-30.
66. Arai, K., et al., *Increase in the glucosylated form of erythrocyte Cu-Zn-superoxide dismutase in diabetes and close association of the nonenzymatic glucosylation with the enzyme activity.* Biochim Biophys Acta, 1987. **924**(2): p. 292-6.
67. Arai, K., et al., *Glycation and inactivation of human Cu-Zn-superoxide dismutase. Identification of the in vitro glycated sites.* J Biol Chem, 1987. **262**(35): p. 16969-72.
68. Kawamura, N., et al., *Increased glycated Cu,Zn-superoxide dismutase levels in erythrocytes of patients with insulin-dependent diabetis mellitus.* J Clin Endocrinol Metab, 1992. **74**(6): p. 1352-4.
69. Fujii, J., et al., *Oxidative stress caused by glycation of Cu,Zn-superoxide dismutase and its effects on intracellular components.* Nephrol Dial Transplant, 1996. **11 Suppl 5**: p. 34-40.
70. Sirangelo, I., et al., *Glycation in Demetalated Superoxide Dismutase 1 Prevents Amyloid Aggregation and Produces Cytotoxic Ages Adducts.* Front Mol Biosci, 2016. **3**: p. 55.
71. Bosco, D.A., et al., *Wild-type and mutant SOD1 share an aberrant conformation and a common pathogenic pathway in ALS.* Nat Neurosci, 2010. **13**(11): p. 1396-403.
72. Martins, D. and A.M. English, *SOD1 oxidation and formation of soluble aggregates in yeast: relevance to sporadic ALS development.* Redox Biol, 2014. **2**: p. 632-9.
73. Zhang, H., et al., *Bicarbonate-dependent peroxidase activity of human Cu,Zn-superoxide dismutase induces covalent aggregation of protein: intermediacy of tryptophan-derived oxidation products.* J Biol Chem, 2003. **278**(26): p. 24078-89.
74. Auclair, J.R., et al., *Post-translational modification by cysteine protects Cu/Zn-superoxide dismutase from oxidative damage.* Biochemistry, 2013. **52**(36): p. 6137-44.

75. Auclair, J.R., et al., *Structural consequences of cysteinylation of Cu/Zn-superoxide dismutase.* Biochemistry, 2013. **52**(36): p. 6145-50.
76. Fujiwara, N., et al., *Oxidative modification to cysteine sulfonic acid of Cys111 in human copper-zinc superoxide dismutase.* J Biol Chem, 2007. **282**(49): p. 35933-44.
77. Ihara, K., et al., *Structural switching of Cu,Zn-superoxide dismutases at loop VI: insights from the crystal structure of 2-mercaptoethanol-modified enzyme.* Biosci Rep, 2012. **32**(6): p. 539-48.
78. Souza, J.M., G. Peluffo, and R. Radi, *Protein tyrosine nitration--functional alteration or just a biomarker?* Free Radic Biol Med, 2008. **45**(4): p. 357-66.
79. Radi, R., *Nitric oxide, oxidants, and protein tyrosine nitration.* Proc Natl Acad Sci U S A, 2004. **101**(12): p. 4003-8.
80. Pacher, P., J.S. Beckman, and L. Liaudet, *Nitric oxide and peroxynitrite in health and disease.* Physiol Rev, 2007. **87**(1): p. 315-424.
81. Yamakura, F. and H. Kawasaki, *Post-translational modifications of superoxide dismutase.* Biochimica Et Biophysica Acta-Proteins and Proteomics, 2010. **1804**(2): p. 318-325.
82. Ischiropoulos, H., et al., *Peroxynitrite-mediated tyrosine nitration catalyzed by superoxide dismutase.* Arch Biochem Biophys, 1992. **298**(2): p. 431-7.
83. Yamakura, F., et al., *Modification of a single tryptophan residue in human Cu,Zn-superoxide dismutase by peroxynitrite in the presence of bicarbonate.* Biochimica Et Biophysica Acta-Protein Structure and Molecular Enzymology, 2001. **1548**(1): p. 38-46.
84. Yamakura, F., et al., *Nitrated and oxidized products of a single tryptophan residue in human Cu,Zn-superoxide dismutase treated with either peroxynitrite-carbon dioxide or myeloperoxidase-hydrogen peroxide-nitrite.* J Biochem, 2005. **138**(1): p. 57-69.
85. Alvarez, B., et al., *Inactivation of human Cu,Zn superoxide dismutase by peroxynitrite and formation of histidinyl radical.* Free Radic Biol Med, 2004. **37**(6): p. 813-22.
86. Taylor, D.M., et al., *Tryptophan 32 potentiates aggregation and cytotoxicity of a copper/zinc superoxide dismutase mutant associated with familial amyotrophic lateral sclerosis.* J Biol Chem, 2007. **282**(22): p. 16329-35.
87. Dewhurst, H.M. and M.P. Torres, *Systematic analysis of non-structural protein features for the prediction of PTM function potential by artificial neural networks.* PLoS One, 2017. **12**(2): p. e0172572.
88. Dewhurst, H.M., S. Choudhury, and M.P. Torres, *Structural Analysis of PTM Hotspots (SAPH-ire)--A Quantitative Informatics Method Enabling the Discovery of Novel Regulatory Elements in Protein Families.* Mol Cell Proteomics, 2015. **14**(8): p. 2285-97.
89. Torres, M.P., H. Dewhurst, and N. Sundararaman, *Proteome-wide Structural Analysis of PTM Hotspots Reveals Regulatory Elements Predicted to Impact Biological Function and Disease.* Mol Cell Proteomics, 2016. **15**(11): p. 3513-3528.
90. Rakhit, R. and A. Chakrabartty, *Structure, folding, and misfolding of Cu,Zn superoxide dismutase in amyotrophic lateral sclerosis.* Biochim Biophys Acta, 2006. **1762**(11-12): p. 1025-37.
91. Doucette, P.A., et al., *Dissociation of human copper-zinc superoxide dismutase dimers using chaotrope and reductant. Insights into the molecular basis for dimer stability.* J Biol Chem, 2004. **279**(52): p. 54558-66.

92. Molnar, K.S., et al., *A common property of amyotrophic lateral sclerosis-associated variants: destabilization of the copper/zinc superoxide dismutase electrostatic loop.* J Biol Chem, 2009. **284**(45): p. 30965-73.
93. Hornberg, A., et al., *The coupling between disulphide status, metallation and dimer interface strength in Cu/Zn superoxide dismutase.* J Mol Biol, 2007. **365**(2): p. 333-42.
94. Rakhit, R., et al., *An immunological epitope selective for pathological monomer-misfolded SOD1 in ALS.* Nat Med, 2007. **13**(6): p. 754-9.
95. Saccon, R.A., et al., *Is SOD1 loss of function involved in amyotrophic lateral sclerosis?* Brain, 2013. **136**(Pt 8): p. 2342-58.
96. Reddi, A.R., et al., *The overlapping roles of manganese and Cu/Zn SOD in oxidative stress protection.* Free Radic. Biol. Med., 2009. **46**: p. 154-62.
97. Sanchez, R.J., et al., *Exogenous manganous ion at millimolar levels rescues all known dioxygen-sensitive phenotypes of yeast lacking CuZnSOD.* J Biol Inorg Chem, 2005. **10**(8): p. 913-23.
98. Elchuri, S., et al., *CuZnSOD deficiency leads to persistent and widespread oxidative damage and hepatocarcinogenesis later in life.* Oncogene, 2005. **24**(3): p. 367-80.
99. Blander, G., et al., *Superoxide dismutase 1 knock-down induces senescence in human fibroblasts.* J Biol Chem, 2003. **278**(40): p. 38966-9.
100. Phillips, J., et al., *Null mutations of copper/zinc superoxide in Drosophila confer hypersensitivity to paraquat and reduced longevity.* Proc. Natl. Acad. Sci. U.S.A., 1989. **83**: p. 3820-3824.
101. Corson, L.B., et al., *Oxidative stress and iron are implicated in fragmenting vacuoles of Saccharomyces cerevisiae lacking Cu,Zn Superoxide dismtuase.* J. Biol. Chem., 1999. **274**: p. 27590-27596.
102. McNaughton, R.L., et al., *Probing in vivo Mn2+ speciation and oxidative stress resistance in yeast cells with electron-nuclear double resonance spectroscopy.* Proc Natl Acad Sci U S A, 2010. **107**(35): p. 15335-9.
103. Papa, L., G. Manfredi, and D. Germain, *SOD1, an unexpected novel target for cancer therapy.* Genes Cancer, 2014. **5**(1-2): p. 15-21.
104. Palomo, G.M. and G. Manfredi, *Exploring new pathways of neurodegeneration in ALS: the role of mitochondria quality control.* Brain Res, 2015. **1607**: p. 36-46.
105. Corson, L.B., Strain, J.J., Culotta, V.C. & Cleveland, D.W., *Chaperone-facilitated copper binding is a property common to several classes of familial amyotrophic lateral sclerosis-linked superoxide dismutase mutants.* Proceedings of the National Academy of Sciences of the United States of America, 1998. **95**: p. 6361-6366.
106. Davies, M.N., et al., *The Acetyl Group Buffering Action of Carnitine Acetyltransferase Offsets Macronutrient-Induced Lysine Acetylation of Mitochondrial Proteins.* Cell Rep, 2016. **14**(2): p. 243-54.
107. Kulej, K., et al., *Time-resolved global and chromatin proteomics during herpes simplex virus (HSV-1) infection.* Mol Cell Proteomics, 2017.
108. Soderblom, E.J., et al., *Quantitative label-free phosphoproteomics strategy for multifaceted experimental designs.* Analytical Chemistry, 2011. **83**(10): p. 3758-64.
109. Hoos, M.D., et al., *Longitudinal study of differential protein expression in an Alzheimer's mouse model lacking inducible nitric oxide synthase.* J Proteome Res, 2013. **12**(10): p. 4462-77.

110. Finn, R.D., et al., *Pfam: the protein families database.* Nucleic Acids Res, 2014. **42**(Database issue): p. D222-30.
111. Edgar, R.C., *MUSCLE: a multiple sequence alignment method with reduced time and space complexity.* BMC Bioinformatics, 2004. **5**: p. 113.
112. Tighe, A., V.L. Johnson, and S.S. Taylor, *Truncating APC mutations have dominant effects on proliferation, spindle checkpoint control, survival and chromosome stability.* J Cell Sci, 2004. **117**(Pt 26): p. 6339-53.
113. Goto, H. and M. Inagaki, *Production of a site- and phosphorylation state-specific antibody.* Nat Protoc, 2007. **2**(10): p. 2574-81.
114. Flohe, L. and F. Otting, *Superoxide dismutase assays.* Methods Enzymol, 1984. **105**: p. 93-104.
115. Ran, F.A., et al., *Genome engineering using the CRISPR-Cas9 system.* Nat Protoc, 2013. **8**(11): p. 2281-308.
116. Hodson, A.E., T.S. Tippetts, and B.T. Bikman, *Insulin treatment increases myocardial ceramide accumulation and disrupts cardiometabolic function.* Cardiovasc Diabetol, 2015. **14**: p. 153.
117. Andersen, J.L., et al., *A biotin switch-based proteomics approach identifies 14-3-3zeta as a target of Sirt1 in the metabolic regulation of caspase-2.* Molecular Cell, 2011. **43**(5): p. 834-42.
118. Mortenson, J.B., et al., *Histone deacetylase 6 (HDAC6) promotes the pro-survival activity of 14-3-3zeta via deacetylation of lysines within the 14-3-3zeta binding pocket.* J Biol Chem, 2015.
119. R. Rakhit, A.C., *Structure, folding, and misfolding of Cu,Zn superoxide dismutase in amyotrophic lateral sclerosis.* Biochimica et Biophysica Acta (BBA), 2006. **1762**(11-12): p. 1025-1037.
120. Lin, Z., Xu, H., Wang, J., Lin, Q., Ruan, Z., Liu, F., Jin, W., Huang, H. & Chen, X., *SIRT5 desuccinylates and activates SOD1 to eliminate ROS.* Biochemical and Biophysical Research Communications 2013. **441**: p. 191-195.
121. Xiong, Y. and K.L. Guan, *Mechanistic insights into the regulation of metabolic enzymes by acetylation.* J Cell Biol, 2012. **198**(2): p. 155-64.
122. Hirschey, M.D. and Y. Zhao, *Metabolic Regulation by Lysine Malonylation, Succinylation, and Glutarylation.* Mol Cell Proteomics, 2015. **14**(9): p. 2308-15.
123. Du, J., et al., *Sirt5 is a NAD-dependent protein lysine demalonylase and desuccinylase.* Science, 2011. **334**(6057): p. 806-9.
124. Nishida, Y., Rardin, M.J., Carrico, C., He, W., Sahu, A.K., Gut, P., Najjar, R., Fitch, M., Hellerstein, M., Gibson, B.W. & Verdin, E., *SIRT5 Regulates both Cytosolic and Mitochondrial Protein Malonylation with Glycolysis as a Major Target.* Molecular Cell, 2015. **59**(2): p. 321-332.
125. Matsushita, N., Yonashiro, R., Ogata, Y. Sugiura, A., Nagashima, S., Fukuda, T., Inatome, R. & Yanagi, S., *Distinct regulation of mitochondrial localization and stability of two human Sirt5 isoforms.* Genes to cells: devoted to molecular & cellular mechanisms, 2011. **16**(2): p. 190-202.
126. Rardin, M.J., He, W., Nishida, Y., Newman, J.C., Carrico, C., Danielson, S.R., Guo, A., Gut, P., Sahu, A.K., Li, Biao, Uppala, R., Fitch, M., Riiff, T., Zhu, L., Zhou, J., Mulhern, D., Stevens, R.D., Ilkayeva, O.R., Newgard, C.B., Jacobson, M.P., Hellerstein, M., Goetzman,

E.S., Gibson, B.W. & Verdin, E., *SIRT5 Regulates the Mitochondrial Lysine Succinylome and Metabolic Networks.* Cell Metabolism, 2013. **18**(6): p. 920-933.
127. Papa, L., Hahn, M., Marsh, E.L., Evans, B.S. & Germain, D., *SOD2 to SOD1 switch in breast cancer.* Journal of Biological Chemistry, 2014. **289**(9): p. 5412-5416.
128. Vijayvergiya, C., Beal, M.F., Buck, J. & Manfredi, G., *Mutant Superoxide Dismutase 1 Forms Aggregates in the Brain Mitochondrial Matrix of Amyotrophic Lateral Sclerosis Mice.* Journal of Neuroscience, 2005. **25**(10): p. 2463-2470.
129. Magrane, J., et al., *Mutant SOD1 in neuronal mitochondria causes toxicity and mitochondrial dynamics abnormalities.* Hum Mol Genet, 2009. **18**(23): p. 4552-64.
130. Kawamata, H.M., G., *Import, Maturation, and Function of SOD1 and Its Copper Chaperone in the Mitochondrial Intermembrane Space.* Antioxidants & Redox Signaling, 2010. **13**(9): p. 1375-1384.
131. Bihlmaier, K., Mesecke, N., Terziyska, N., Bien, M., Hell, K. & Herrmann, J.M., *The disulfide relay system of mitochondria is connected to the respiratory chain.* Journal of Cell Biology, 2007. **179**(3): p. 389-395.
132. Takeshige, K. and S. Minakami, *NADH- and NADPH-dependent formation of superoxide anions by bovine heart submitochondrial particles and NADH-ubiquinone reductase preparation.* Biochem J, 1979. **180**(1): p. 129-35.
133. Raha, S. and B.H. Robinson, *Mitochondria, oxygen free radicals, disease and ageing.* Trends Biochem Sci, 2000. **25**(10): p. 502-8.
134. Fischer, L.R., et al., *SOD1 targeted to the mitochondrial intermembrane space prevents motor neuropathy in the Sod1 knockout mouse.* Brain, 2011. **134**(Pt 1): p. 196-209.
135. Sturtz, L.A., et al., *A fraction of yeast Cu,Zn-superoxide dismutase and its metallochaperone, CCS, localize to the intermembrane space of mitochondria. A physiological role for SOD1 in guarding against mitochondrial oxidative damage.* J Biol Chem, 2001. **276**(41): p. 38084-9.
136. Kawamata, H. and G. Manfredi, *Different regulation of wild-type and mutant Cu,Zn superoxide dismutase localization in mammalian mitochondria.* Hum Mol Genet, 2008. **17**(21): p. 3303-17.
137. Reddehase, S., et al., *The disulfide relay system of mitochondria is required for the biogenesis of mitochondrial Ccs1 and Sod1.* J Mol Biol, 2009. **385**(2): p. 331-8.
138. Jacobson, J., et al., *Induction of mitochondrial oxidative stress in astrocytes by nitric oxide precedes disruption of energy metabolism.* J Neurochem, 2005. **95**(2): p. 388-95.
139. Zorov, D.B., M. Juhaszova, and S.J. Sollott, *Mitochondrial reactive oxygen species (ROS) and ROS-induced ROS release.* Physiol Rev, 2014. **94**(3): p. 909-50.
140. Longo, V.D., E.B. Gralla, and J.S. Valentine, *Superoxide dismutase activity is essential for stationary phase survival in Saccharomyces cerevisiae. Mitochondrial production of toxic oxygen species in vivo.* J Biol Chem, 1996. **271**(21): p. 12275-80.
141. Kelly, B., et al., *Metformin Inhibits the Production of Reactive Oxygen Species from NADH:Ubiquinone Oxidoreductase to Limit Induction of Interleukin-1beta (IL-1beta) and Boosts Interleukin-10 (IL-10) in Lipopolysaccharide (LPS)-activated Macrophages.* J Biol Chem, 2015. **290**(33): p. 20348-59.
142. Ouslimani, N., et al., *Metformin decreases intracellular production of reactive oxygen species in aortic endothelial cells.* Metabolism, 2005. **54**(6): p. 829-34.

143. Marycz, K., et al., *Metformin Decreases Reactive Oxygen Species, Enhances Osteogenic Properties of Adipose-Derived Multipotent Mesenchymal Stem Cells In Vitro, and Increases Bone Density In Vivo.* Oxid Med Cell Longev, 2016. **2016**: p. 9785890.
144. Lenaz, G., et al., *Mitochondrial Complex I: structural and functional aspects.* Biochim Biophys Acta, 2006. **1757**(9-10): p. 1406-20.